Laboratory of Geo-Information Science and Remote Sensing
(minor MSc thesis report)

Mapping Forest Degradation in the Mau Forest Complex Using NDFI Time Series

Tom Bewernick

August 2016

Supervision:

Mariana Rufino (CIFOR), Brice Mora (Wageningen UR)

WAGENINGEN UNIVERSITY
WAGENINGEN UR

CIFOR

Mapping Forest Degradation in the Mau Forest Complex Using NDFI Time Series

Tom Bewernick

Registration number 880312064060

Supervisors:

Brice Mora, Laboratory of Geo-information Science and Remote Sensing, Wageningen University

Mariana Rufino, Center for International Forestry Research

A thesis submitted in partial fulfilment of the degree of Master of Science at Wageningen University and Research Centre, The Netherlands.

Date: 11.08.2016

Wageningen, The Netherlands

Wageningen University and Research Centre
Laboratory of Geo-Information Science and Remote Sensing

Acknowledgements

In genuine love, I would like to express my gratitude to all the people and circumstances that brought me here to this moment of finishing my MSc program. I am especially thankful for all the wonderful insights beyond my thesis research in this demanding period.

Thank you, Brice Mora and Mariana Rufino for dedicating your precious time for my supervision. Your open and creative minds provided valuable guidance throughout this thesis. A special thanks also to Salome Chelelgo head of the Kenyan Wildlife Service department in Kericho, who offered valuable support during my field work in Kenya. Thank you Malibe, Koech, Rono, Bonface, Philamon, Stanley, Raban and my brother Myamagi, without whom I could not make it through the forest. You made me laugh and understand some of the Kenyan ways.

Throughout this thesis I further gained valuable technical support from Michael Schulz, Loic Dutrieux, Eliakim Hamunyela and Erik van Schaik. Thank you all for sharing your collective knowledge with me. I hope your willingness for collaboration will accelerate the field of remote sensing as a whole. Thanks also to the R community for providing countless tutorials, hints and powerful software packages. Without you I could not develop the scripts to perform this research. This thesis exemplifies how open software initiatives contribute to knowledge dispersal in society.

Thank you Clemmie for putting my mind at so much ease after long days in the office. What an angel you are. Thanks also to my housemates and beautiful neighbours that brought a lot of joy and laughter throughout the finalization of my minor thesis. I also want to express my gratitude to my mother, sister and father for their constant unconditional support. Without you I certainly wouldn't be here. I hope that the finalization of my study will bring us closer again.

Abstract

Located in a highly populated region the Kenyan Mau forest complex is increasingly exploited for cattle grazing, fuel wood collection and charcoal burning. This has big implications on the state of the forest as the understorey is disturbed and tree cover gradually diminishes. To understand the underlying forces driving forest degradation knowledge of the timing and location of anthropogenic disturbances in the forest is crucial. Using a stable forest mask for the period between 2000-2016 the analysis was limited to persistently forested areas, thus excluding deforestation. To detect forest degradation, we computed time series from the Normalized Difference Fraction Index (NDFI) which synthesizes subpixel fraction images from spectral mixture models. NDFI time series were then screened for structural changes using the data-driven Breaks For Additive Season and Trend (BFAST) model. Our results indicate an overall detection accuracy of 75.74 %. User and Producer accuracies for the mapped forest degradation class amounted 84.31% and 56.58% respectively. The no-degradation class showed user and Producer accuracies of 72.03% and 91.4% respectively. Undetected degradation patches generally remained below an area size of 0.2 ha, which reveals the importance of matching targeted degradation processes with an appropriate spatial sensor resolution. Furthermore, the year 2015 indicated an exceptional peak of degradation processes. In that year about 28 % of non-disturbed forest samples were falsely attributed as degraded. 2015 stands out with the lowest precipitation rates among all years in the study period, likely leading to the false identification of phenological anomalies as actual degradation processes. The main benefit of combining NDFI time series and BFAST is the high sensitivity towards canopy changes. Potentially, the employed change detection method can be further enhanced using additional spectral indices and breakpoint validation criteria that are more resilient to fluctuations of climate and vegetation phenology. While revealing some weaknesses of the approach the study also mapped hotspots of forest degradation in the Mau forest. These findings are relevant for the daily work of local forest services but also for future research and continued degradation mapping.

Keywords: Remote sensing, Landsat, Forest degradation, Spectral mixture analysis, Normalized Difference Fraction Index, BFAST

Table of contents

List of Tables

List of Figures

List of Annexes

Abbreviations

MFC	Mau Forest Complex
REDD+	Reducing emissions from deforestation and forest degradation in developing countries; and the role of conservation, sustainable management of forests and enhancement of forest carbon stocks in developing countries
MRV	Measuring Reporting and Verification
LC	Land cover
LCC	Land cover change
RS	Remote Sensing
SMA	Spectral mixture analysis
GV	Green Vegetation
NPV	non-photosynthetic vegetation
NDFI	Normalized Difference Fraction Index
USGS	U.S. Geological Survey
TM	Thematic Mapper (sensor on Landsat 5)
ETM+	Enhanced thematic mapper (sensor on Landsat 7)
OLI	Operational Land Imager (sensor on Landsat 8)
TS	Time series
TSS	Time Series Stacks
WRS	Worldwide Reference System
SLC	Scan Line Corrector
LEDAPS	Landsat Ecosystem Disturbance Adaptive Processing System

1 Introduction

1.1 Background

The Mau forest complex (MFC) is part of the largest closed-canopy montane forest ecosystem in Eastern Africa (Were, Dick and Singh 2013). While these forests represent an important sanctuary for the Kenyan flora and fauna, they are also major sinks of CO_2 (Vidal 2009). Furthermore, the MFC provides a wide range of Ecosystem Services such as the improvement of soil fertility through supporting nutrient cycling, local climate regulation, flood prevention and rainwater retention (Imo 2012). The latter is particularly important for local livelihoods as it contributes to year-round water availability, even throughout the dry season (Mogaka et al. 2006).

Located in a highly populated region of western Kenya, the MFC underwent continuous processes of uncontrolled forest degradation (Imo 2012). Given varying degrees of poverty, local livelihoods rely on land for settlement, cultivation and livestock grazing. Due to high demographic pressure along the edges of the MFC, forest resources are increasingly exploited for cattle grazing, fuel wood collection and charcoal burning. Although the structure and composition of the forest is modified by these activities the respective areas are not considered as deforested because the original land cover (LC) is not replaced.

Beside the local and regional importance of the MFC, tropical forest degradation is also acknowledged as a relevant aspect of the international climate change agreement (UNFCCC, 2015). Attributing carbon stock changes to forest degradation poses a big challenge in advancing mechanisms for carbon payments through REDD+[1]. For the implementation at national level, changes in carbon stocks have to be adequately monitored as required for national Measuring Reporting and Verification (MRV) systems. That specifically demands the acquisition of so-called activity data, i.e. the quantified area undergoing forest change processes (deforestation, forest degradation and regrowth). While few deforestation monitoring systems exist, forest degradation is not monitored regularly in any tropical country. This however is needed to support the Kenyan MRV systems and to track illegal logging activities (Sharife 2010). Furthermore, better knowledge on the various drivers of forest degradation can help to mitigate societal needs and shape adequate policies to protect the MFC and tropical forests at large.

1.2 Problem definition

Currently, no common definition of forest degradation exists. Depending on the perspective, many biophysical processes can indicate a form of degradation (e.g. soil degradation, biodiversity loss etc.). In the context of climate change, forest degradation can be defined as a loss of carbon stocks without land cover change (LCC). Compared to other degradation processes, loss of carbon stocks can be directly related to logging activities and fire, which

[1] REDD+ poses an incentive mechanism to "reduce emissions from deforestation and degradation and to conserve and enhance carbon stocks".

manifests in canopy cover changes. Multi-temporal optical Remote Sensing (RS) imagery can be employed to map such processes over time (Broich et al. 2011). However, this is far more challenging than mapping deforestation as degraded forest 'pixels' represent complex environments with different features on the ground (i.e. vegetation, dead trees, bark, tree branches, soil, shade) (Souza and Roberts 2005). To differentiate natural degradation processes from anthropogenic causes, many approaches additionally incorporate bare soil fraction per pixel, as main drivers charcoal burning and timber extraction are characterized by the complete removal of biomass (Gaveau et al. 2014, Hirschmugl et al. 2014, Souza, Roberts and Cochrane 2005). Due to the ephemeral nature of RS signals and the spectral ambiguity between low intensity logging and intact forests, automated pixel-based approaches are needed that exploit the full temporal and spectral coverage of a sensor (Asner, Keller and Silva 2004). The use of spectral mixture analysis (SMA) (Stueve et al. 2009), a technique based on modelling image spectra as the linear combination of pure spectra (Adams, Smith and Gillespie 1993), has been a great advancement for the mapping of forest degradation (Souza et al. 2005). While SMA-derived fractions of shade and Green Vegetation (GV) are helpful to identify canopy gaps (Asner et al. 2002), the bare soil fraction allows to identify skid trails and logging roads (de Wasseige and Defourny 2004). Souza et al. (2005) developed a spectral index that incorporates relevant endmember fractions in degrading forest landscapes, the Normalized Difference Fraction Index (NDFI).

Current change detection approaches use the NDFI and SMA-derived fraction images for the classification of few images and comparing them over time (Sofan et al. 2016, Souza Jr et al. 2013). Although this method generated satisfactory results in Brazil and Indonesia (ibid.), a few disadvantages can be identified for applying the method in the MFC. Forests in Kenya show a higher seasonality than rainforest, which can result in the confusion of forest classes if bi-temporal imagery from different seasons are compared (Coppin et al. 2004). Furthermore, degradation is not detectable anymore within 1 year due to understorey regrowth (Souza et al. 2005). Recently, a number of time-series based approaches for change detection have been developed (e.g. Verbesselt et al. 2010b, Verbesselt et al. 2012, Zhu and Woodcock 2012). This follows a general trend towards multi-temporal change detection, exploiting the full temporal detail of the RS-based data streams available today (Hansen and Loveland 2012). In part this is motivated by recent changes in the data policy of the U.S. Geological Survey (USGS) and advancements in pre-processing algorithms permits to harness the full Landsat archive (Wulder et al. 2012). The spectral coverage and spatial resolution of Landsat imagery allows to track both tree cover changes and primary logging roads, which makes it a promising data source for mapping forest degradation (Broich et al. 2011, Gaveau et al. 2014, Margono et al. 2012). Some change detection approaches are fully data-driven and therefore require no training data or detailed knowledge of the expected change. The pixel-based Breaks For Additive Season and Trend (BFAST) Monitor method developed by Verbesselt, Zeileis and Herold (2012) has been previously used to detect small-scale disturbances in montane forests in Ethiopia (DeVries et al. 2015). BFAST is robust in regard of short-term data variations and inherent noise (e.g. clouds and atmospheric scatter), which further supports its use in tropical areas (Verbesselt et al. 2010b).

Given the necessity to enhance forest monitoring in the MFC, the main objective of this project was to develop a method for the timely detection of forest degradation combining NDFI TS and BFAST. In this context, it was hypothesized that RS TS can be partitioned in such a way that they are representative of forest degradation processes. Computed degradation maps will support the Initiative for Sustainable Landscapes (ISLA) Program operating in South West Mau to develop a baseline, and to assess proposed interventions.

2 Study area

The study site for mapping forest degradation stretches from the western parts of the MFC to the eastern shorelines of Lake Victoria covering mainly the south-central part of the Rift Valley province (see Figure 1). The area is designated by 1735 mm annual precipitation at an average temperature of 18.1°C (Acker, J. G. & G. Leptoukh 2007). Ranging from an altitude between 1,800 - 3,000 m.a.s.l. the forested mountains function as one of the main water towers in Kenya forming the headwaters of the Sondu and Mara catchments. As such this region functions as an important water retention basin supporting agriculture, hydropower generation, urban drinking water supply, and rural livelihoods throughout significant parts of western Kenya.

Forest degradation processes in the study area can be largely attributed to increasing population pressure which manifests in the growing exploitation of forest resources. Lack of governance and poor regulatory policies in the past led to the excision of vast forest areas for settlements, commercial tea and wheat production (Allaway, 1989, unknown, 2002). Despite renewed political efforts against human encroachment, forest destruction continues, especially through the burning of charcoal, one of the cheapest household energy sources in Kenya (GFC 2010, WildlifeDirect 2010). Frequently, degrading forests are soon converted into areas of subsistence agriculture or pastures (Olang and Kundu 2011).

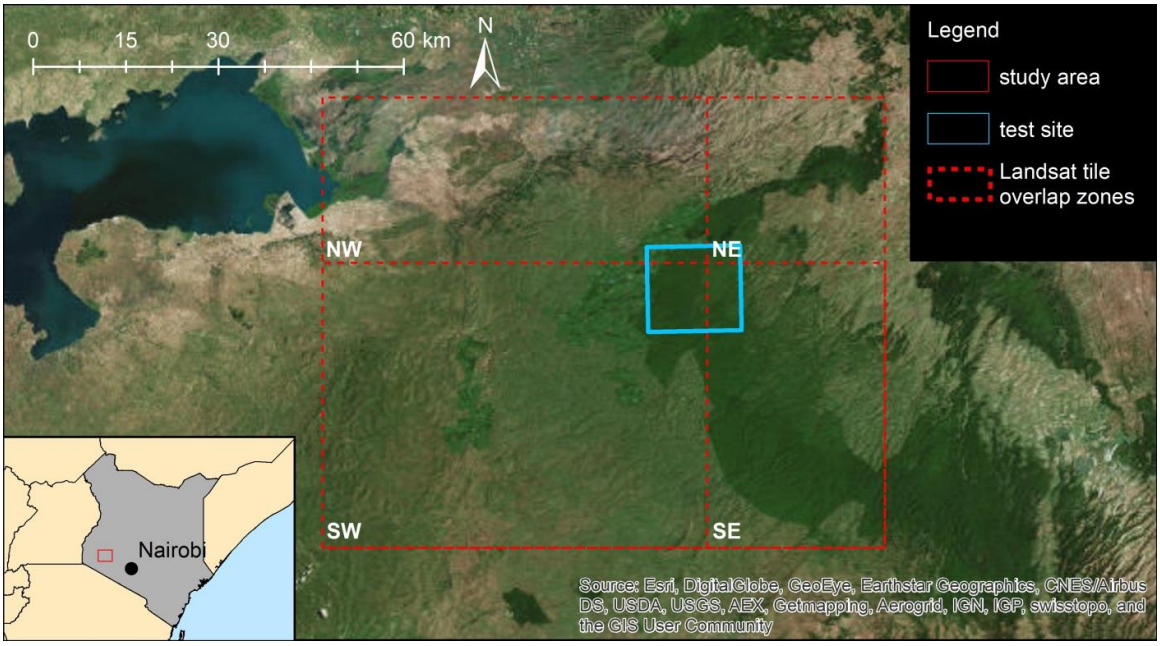

Figure 1: Study area in Kenya

3 Methodology

3.1 Remote sensing data and pre-processing

Optical RS data for this study was comprised of Landsat surface reflectance images from TM (Thematic Mapper), ETM+ (Enhanced Thematic Mapper) and OLI (Operational Land Imager) sensors, provided by the USGS, for the period between 01.01.2000 – 01.07.2016. Imagery with less than 80% cloud cover was downloaded via the ESPA ordering interface (https://espa.cr.usgs.gov). Using the provided metadata, all scenes with a geometric accuracy below 15 m or without any accuracy information were discarded from the dataset. Clouds were flagged using the available FMASK band (Zhu and Woodcock 2012). A full flowchart of implemented pre-processing steps is given in Annex 1.

3.2 Normalized Difference Fraction Index

For an optimal detection of forest canopy disturbance Landsat surface reflectance bands were first used to model sub-pixel fractions (endmembers) of green vegetation (GV), non-photosynthetic vegetation (NPV), bare soil and shade. For that purpose a Spectral Mixture Analysis (Stueve et al. 2009, Adams et al. 1993) was employed using the IMGtools software package developed by Souza et al. (2005). For the accurate modelling of pixel endmember fractions in degraded forests, an optimal identification of pure training spectra (100% GV, NPV, bare soil or shade) is imperative. In this study, we made use of a spectral library specifically developed for endmembers in degraded forest landscapes (Souza et al. 2005).

To enhance the sensitivity of this information towards forest degradation subpixel fractions of endmembers were synthesized into the Normalized Difference Fraction Index (NDFI), which was used successfully for the detection of tropical rainforest degradation (ibid.) (see eq.1).

$$NDFI = \frac{GV_{Shade} - (NPV + Soil)}{GV_{Shade} + NPV + Soil} \quad (1)$$

Where GV_{Shade} is the shade-normalized GV fraction (see eq. 2).

$$GV_{Shade} = \frac{GV}{100 - Shade} \quad (2)$$

3.3 Construction of Time Series Stacks (TSS)

Sequences of Landsat images were bundled into ready-to-use Time Series Stacks (TSS). TSS are acquired at nominal temporal intervals for a specific Worldwide Reference System (WRS) location and enable the pixel-wise computation of any type of TS analysis (Huang et al. 2009). With the implementation of LEDAPS processing prior to the publication of downloadable data, the production of TSS including data of Landsat TM, ETM+ and OLI sensors is a fairly straightforward procedure.

However, one important drawback of Landsat data is the low temporal resolution. Despite the revisit time of 16 days, persistent cloud coverage limits the availability of valid surface reflectance data. Therefore less, often temporally isolated, observations are recorded for the

rainy season. Moreover, the malfunction of the Scan Line Corrector (SLC) in 2003 causes systematic data gaps in all Landsat 7 images, which were used in this study.

In order to enhance the frequency of observations in TSS, the tile overlap of Landsat imagery with neighbouring WRS locations was harnessed. Four overlap zones were defined, each with a unique set of overlapping images (see Figure 1). The extent of each zone was outlined manually. Minima/maxima of x and y coordinates of zone extents were determined visually and are documented in Annex 2. Overlapping images were then cropped (and/or extended) to the extent of each overlap zone and stacked producing one TSS for each spectral band and NDFI in each respective overlap zone. Through this procedure many additional observations were gained, especially for years 2013-2015 (see Figure 2). The zone defined as "NE" displays the amount of data that would be available without the inclusion of neighbouring tiles.

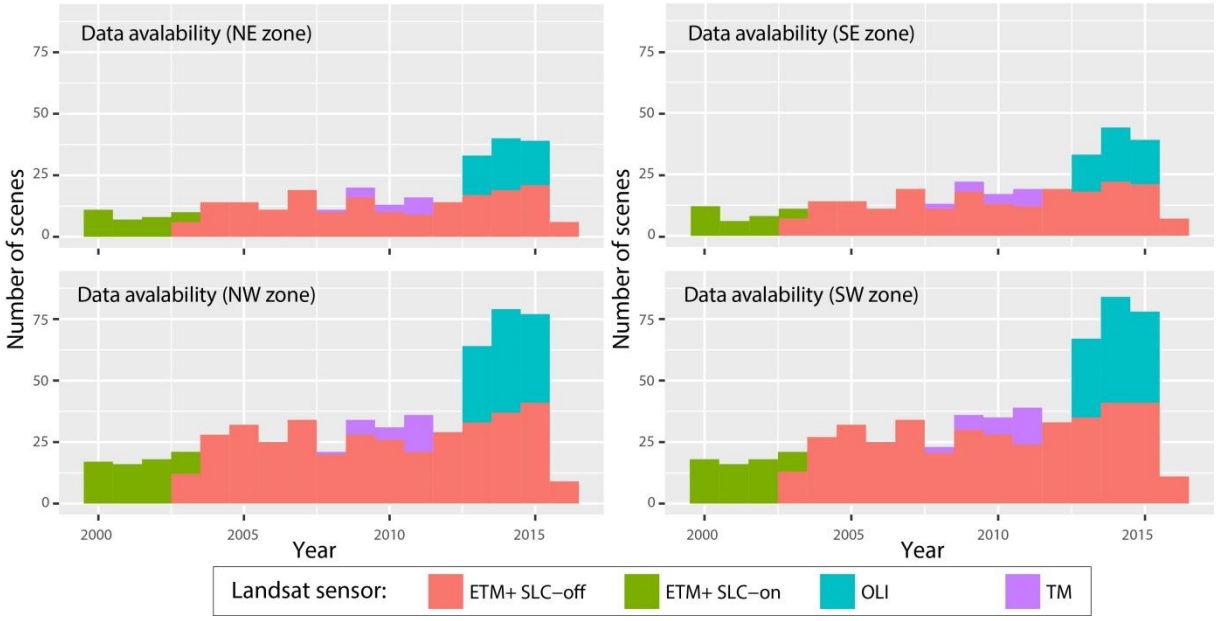

Figure 2: Overlap zones of Landsat images from different WRS tiles

3.4 Noise removal from NDFI TSS

Although Landsat data was provided with an available cloud and cloud shadow mask, not all contaminations were captured. Consequently, NDFI TS are characterized by positive and negative outliers increasing the risk of commission errors (false detection of forest disturbances) (DeVries et al. 2015). Global outlier thresholds (i.e. standard deviation of TS observations) are not applicable for forest change monitoring as these are likely to misinterpret actual changes as outliers. In this study outliers were determined by a moving window through pixel TS, checking if any observation is bigger than 2.5% (positive outliers, mainly cloud shadows) or smaller than 3.5% (negative outliers, mainly clouds) the value of neighbouring observations. These thresholds have been qualitatively assessed using NDFI and FMASK images. Although consecutive outliers cannot be detected by this method, random observation of pixel TS did not reveal frequent abundance of this condition. The resulting TS of this method is exemplified in Figure 3.

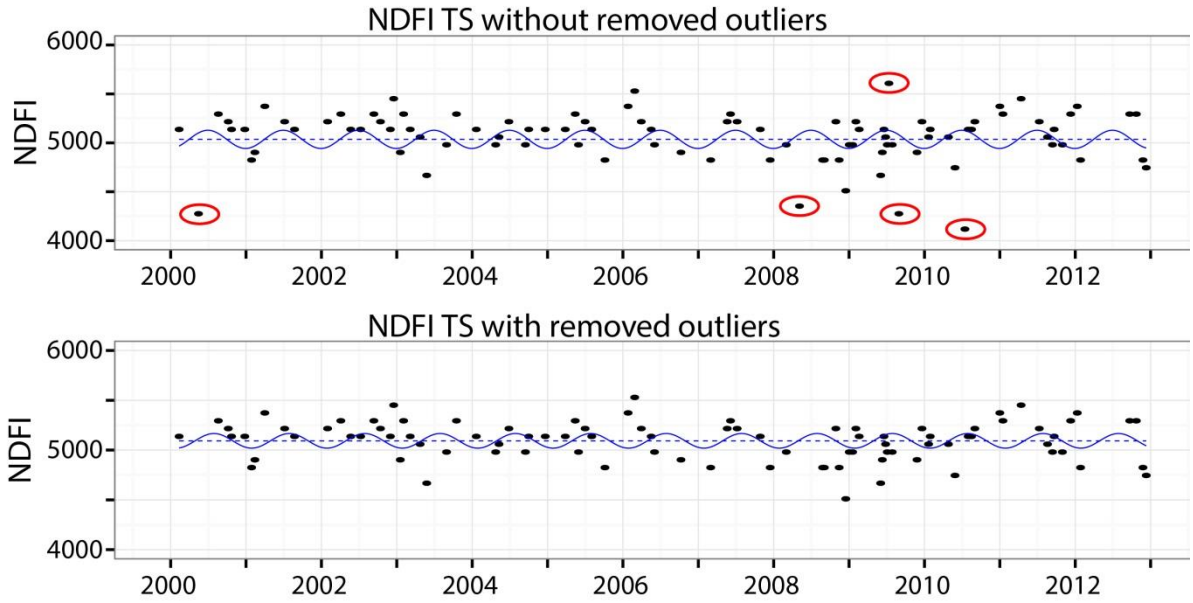

Figure 3: Effect of outlier removal on NDFI TS

3.5 Stable forest mask

Compared to deforestation forest degradation does not describe persistent LCC. In order to disentangle both processes two forest masks were produced for the years 2000 and 2016. By flagging only pixels that are forested in both time steps, degradation monitoring was limited to pixels which are known to be forested throughout the whole study period.

A pixel-wise Random Forest classifier using temporal metrics as input variables was implemented following the procedure described in Griffiths et al. (2013). Temporal metrics were derived from all spectral bands for the periods between 15.04.2000-14.04.2001 and 15.04.2015-14.04.2016. Additional temporal metrics were computed for rainy and dry seasons (see Figure 4). The computed image stacks can be conceptualized as extended snapshots which complement each other by specifying particular seasonal or annual characteristics of spectral indices. Such temporal compositing approaches increase the separability of classes, specifically for forests, pastures and cropland (Griffiths et al. 2013). Furthermore this method is less affected by cloud cover in single images allowing for an area-wide characterization of annual/seasonal states of LC.

The classifier was implemented in supervised mode using reference data derived from aerial photography and Spot imagery. Aerial photography was provided by Rhino Ark for the year 2003. Aerial photos were compared with Landsat imagery from the year 2000 and 2003. As the target year of the first forest mask was 2000, only large, homogenous LC patches with unchanged spectral signatures between 2000 and 2003 were chosen as training sites. Spot imagery was provided by Airbus Defence and Space for the year 2016. To build the second forest mask a linear reference grid resembling Landsat pixels was laid on top of Spot imagery. For most classes, only pixels with homogenous LC were chosen to train the classifier. To conform to the forest definition of the FAO, forested training pixels with different canopy cover (10-100 %) were uniformly collected. Canopy cover was determined visually based on the reference grid.

Initial LC classes comprised pastures, crops, urban, water bodies and wetlands. In a subsequent step these classes were fused into the non-forest class. The forest class consists of primary and secondary forest, shady forest in mountain ridges and tree plantations. In order to focus the analysis on actual forests all spatially isolated clusters of forest with a size below 5 Landsat pixels (4.500m²) were excluded from the forest class.

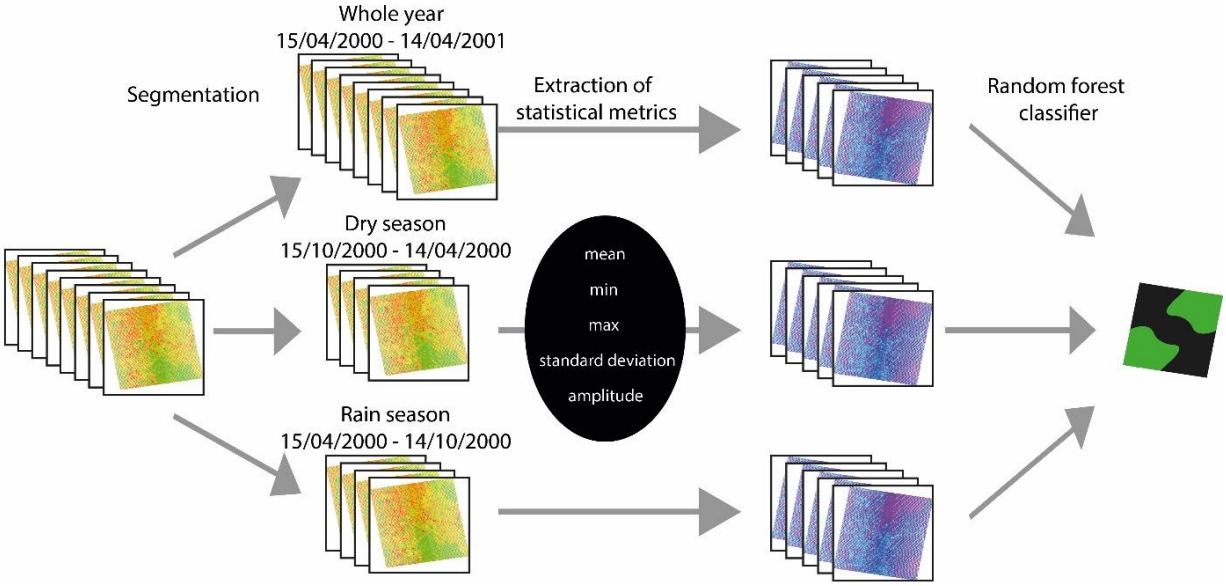

Figure 4: Conceptualization of classification approach to generate forest masks

3.6 Detection of forest degradation

The specific goal of this study was to differentiate two forest states: no-change and degradation. To identify these states a data-driven approach based on the BFAST monitoring algorithm (Verbesselt et al. 2012) was implemented. BFAST fits a model nesting both seasonal signal variations (harmonic) and long term trends (linear) within a defined historical period of stable forest. In our study, the stable history was defined for the years 2000-2010. To detect structural breakpoints in the TS moving sums (MOSUM) of residuals of observations following this stable history period (monitoring period) were computed (ibid.). A breakpoint is declared when residuals and hence also their MOSUM values deviate from 0 at a significance level of 0.05 (see Leisch, Hornik and Kuan (2000)) for more information on this boundary condition). The BFAST approach is described in more detail in Verbesselt et al. (2012).

In order to incorporate the maximum number of observations for fitting the harmonic model, sequential monitoring periods of one year were defined. In case a monitoring year did not demonstrate structural changes in the TS, that year was added to the stable history and the model re-fit. Limiting the length of the monitoring period to one year has the additional advantage that MOSUM values are not affected by observations long after actual change events.

This approach is based on the methods implemented by DeVries et al. (2015) who robustly mapped small-scale forest disturbances in Kafa, Ethiopia. Also based on their experience the

trend term of the algorithm was omitted and solely a first-order harmonic model was fit to the data in the history period (see eq.3). The overall approach is illustrated in Figure 5.

$$y_t = \gamma \sin\left(\frac{2\pi t}{f} + \delta\right) + \varepsilon_t \quad (3)$$

3.7 Disturbance magnitude and soil fraction change thresholds

To ensure the exclusion of spurious breakpoints (due to outliers, seasonal shifts or positive canopy cover changes), two additional aspects were included in the computation. As a measure of change magnitude the median difference between actual and expected NDFI observations was computed within a specified period (see Table 1) of after a detected break (DeVries et al. 2015). Based on the logic that human induced forest degradation is inherently linked with soil exposure (e.g. emergence of paths, biomass removal) an additional validity check using the SMA-derived bare soil fraction images was implemented (Souza et al. 2005). Soil fraction TS were 1) split into pre- and post-disturbance segments around computed breakpoints, 2) the median was calculated separately for observations within each segment and 3) the difference between these medians computed.

A random subset of collected field observations was used to calibrate the parameters listed in Table 1. In 250 iterations parameters were sampled randomly from a uniform distribution. Field observations were used to assess the model performance for each set of parameters. The parameter configuration yielding the highest overall model accuracy was used for the area-wide implementation of the change detection algorithm. During the computation breaks were excluded if either magnitude or soil fraction change thresholds were not exceeded. In these cases the model would omit observations in the period the change magnitude was calculated and the model re-fitted.

Table 1: Parameters to for approval of detected breaks by BFAST model

Parameter	Value
Minimum change magnitude threshold	-0.0354
Post-break period for which to calculate change magnitude	128 d
Minimum bare soil fraction increase	0.31%
Pre- and post-break period for which to calculate soil fraction increase	146 d

All analytical steps were implemented using mainly the “BfastSpatial” and “bfast” packages in R (R Core Development Team 2015, Dutrieux, DeVries and Verbesselt 2014, Verbesselt et al. 2010a).

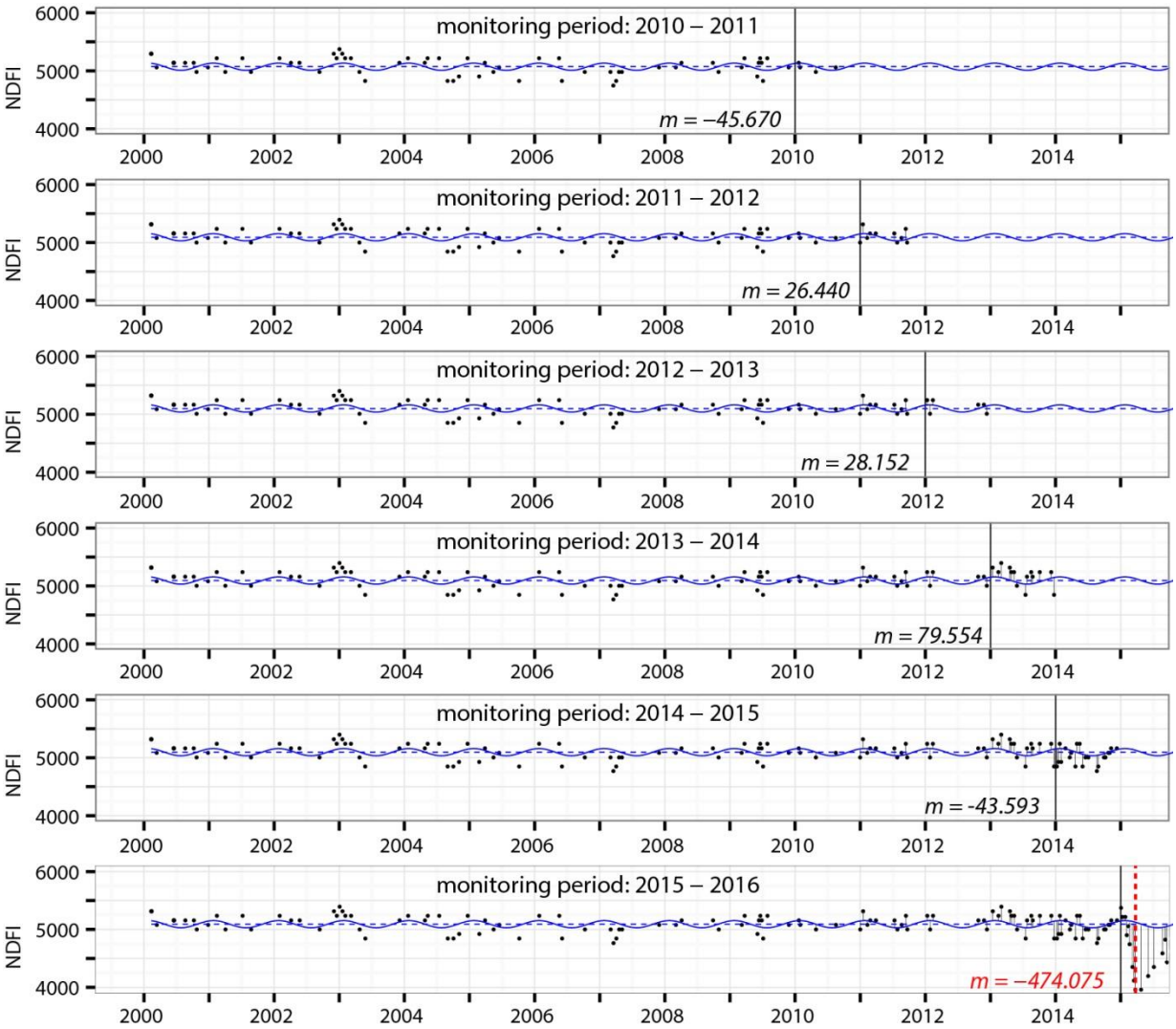

Figure 5: Conceptualization of sequential BFAST monitoring approach

3.8 Accuracy assessment

Forest degradation can be difficult to detect and characterize using imagery only, especially when single trees are removed from forests with a high biomass or high vegetation density. To overcome the limitations of RS based reference datasets, the validation of our method was based on field data. Field data was collected during March-April 2016 in the area indicated in Figure 1. To ensure the visibility of degradation processes the validation was centered on changes in 2014 and 2015. For efficient data collection, mobile devices with integrated GPS and camera functionality were used. The decision-based data collection application of (Pratihast et al. 2014, Pratihast et al. 2013) was adopted for the purpose of this study using the Open Data Kit (ODK) Collect application. An overview of the procedures related to sampling and accuracy assessment can be found in Annex 3.

3.8.1 Sample-based field data

For the sampling itself, a two-stage approach was taken. First accessible forest areas and paths were explored during 7 full days of scrutinizing the inside of the forest. The route was planned as such as to cover 'undisturbed' and degraded parts of the forest as well as bamboo forest. Alongside activity data on forest degradation was documented wherever observed. Harnessing the gained knowledge of the forest a buffer of 100 m was created around accessible forest areas. Following the assumption that most disturbances take place in the vicinity of accessible areas, the second sampling campaign was limited to areas within this buffer. To enhance data collection a stratified random sampling approach was designed using strata derived from preliminary data-driven BFAST outputs. These outputs specify pixels with change and no change as well as magnitude thresholds. Accordingly, strata represent no change and change while the latter was further split into three magnitude classes (low = 0-0.04; medium = 0.04-0.08; high = > 0.08). This differentiation was necessary to calibrate magnitude thresholds of BFAST (see section 3.6).

Given the large prevalence of the non-disturbance class it would have been difficult to derive a reliable estimate of omission errors using only randomly sampled strata derived from BFAST. In our approach that was anticipated by combining purposive activity data collection, with stratification in the proximity of paths (Pfaff 1999). An overview of all collected samples is given in Figure 6.

3.8.2 Validation

The accuracy of the developed change detection method was assessed by comparing final change maps with the collected field data. For the validation only degradation and non-degradation samples of the year 2015 have been compared with change maps. If a breakpoint was detected in the same year as actual disturbances the change was considered correctly identified. Similarly it was considered correct, if no break was detected in that year and the pixel was sampled as non-degraded. Validation results were compiled in a confusion matrix from which classical accuracy measures were derived: overall accuracy, as well as class-specific user and producer accuracies (Congalton 1991).

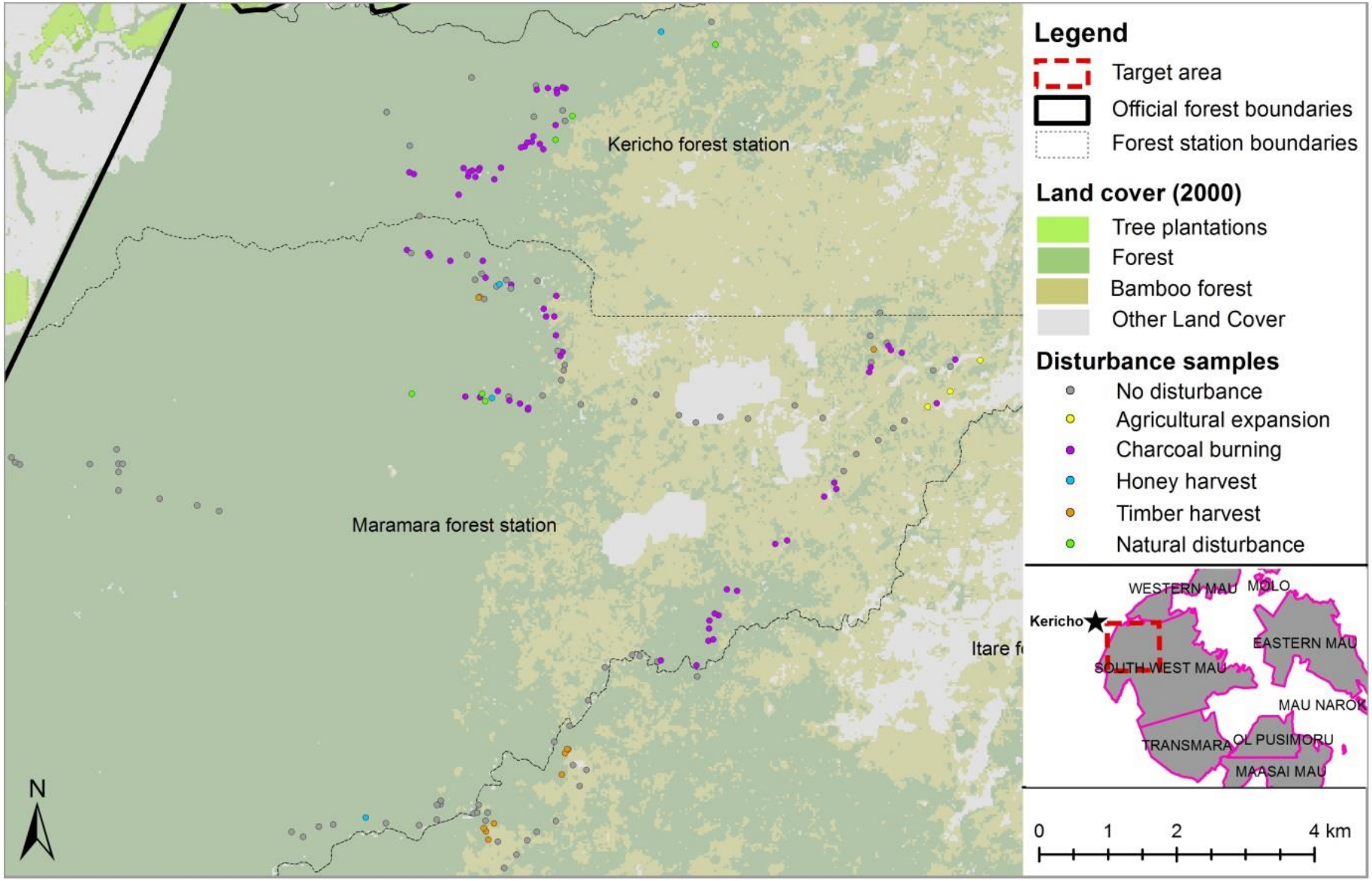

Figure 6: Sampling locations

4 Results and Discussion

4.1 Stable forest mask

Because the forest masks for the years 2000 and 2016 were independent from each other, the accuracy of the final stable forest mask (see Annex 4) was assessed by multiplying User and Producer accuracies for the individual forest masks of 2000 and 2016. Accuracies (estimated with a confidence interval of 95%) and confusion matrices for forest masks of individual years and the stable forest mask are given in Table 2. The final stable forest mask demonstrates a very high overall accuracy around 99.36%.

Table 2: Count-based confusion matrix comparing validation pixels with computed forest masks

Forest mask 2000							
		Reference					
		Forest	Non-forest	Σ	User accuracy (%)	Producer accuracy (%)	Total accuracy (%)
Predicted	Forest	8509	21	8530	99.75	99.46	
	Non-forest	46	6196	6242	99.26	99.66	
	Σ	8555	6217	14705			**99.55 (± 0.13)**
Forest mask 2016							
		Reference					
		Forest	Non-forest	Σ	User accuracy (%)	Producer accuracy (%)	Total accuracy (%)
Predicted	Forest	6889	2	6891	99.97	99.59	
	Non-forest	28	8987	9017	99.66	99.98	
	Σ	6917	8989	15876			**99.81 (± 0.08)**
Stable forest mask							
					User accuracy (%)	Producer accuracy (%)	Total accuracy (%)
				Forest	99.72	99.05	
				Non-forest	98.92	99.64	
							99.36 (± 0.1)

4.2 Annual change maps and accuracy assessment

In the framework of this study the feasibility of combining NDFI TS and BFAST for forest degradation monitoring has been tested. It is the first time this method has been used in mixed evergreen-semi-deciduous forests (Obare and Wangwe 1998) and in the context of forest degradation. The main outputs of this work are forest degradation maps shown in Annex 5.

Overall the method performed at an adequate accuracy. A confusion matrix, including quantified accuracies (confidence interval = 95%), comparing collected field samples with degradation maps is given in Table 3.

Table 3: Count-based confusion matrix comparing field observations with computed forest degradation maps

		Reference					
		No-Degradation	Degradation	Σ	User accuracy (%)	Producer accuracy (%)	Total (%)
Predicted	No-degradation	85	33	118	72.03	91.40	**75.74 (± 7.0)**
	Degradation	8	43	51	84.31	56.58	
	Σ	93	76	169			

From the confusion matrix, we estimated a total accuracy 75.74 %. User and Producer accuracies for the mapped forest degradation class amount 84.31% and 56.58% respectively. The no-degradation class showed user and Producer accuracies of 72.03% and 91.4% respectively.

A comparison of the annual degradation maps indicates a peak of degradation processes in 2015, while least disturbances took place in 2013 (see Figure 7). The big difference between 2015 and other years is discussed in section 4.3.

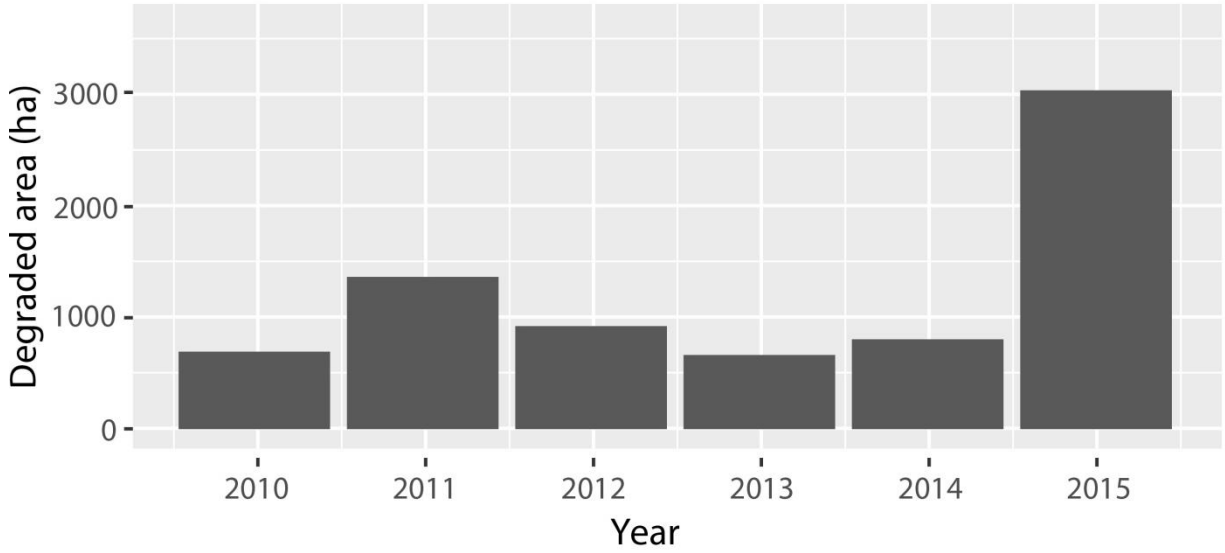

Figure 7: Annual forest degradation in hectares (2010-2015)

Figure 8 composites detected disturbances of all monitoring years in one map. Hotspots of degradation processes are concentrated in the forest stations of Chepsil, the central part of Kericho and the eastern parts of MaraMara. The maps indicate different spatial patterns of forest degradation. While degradation areas in the Chepsil district cover large coherent areas, disturbed areas in Kericho, MaraMara and Itare are much smaller and patchier. Observations during field work indicated that the main driver of forest degradation in these areas is charcoal burning and that kilns are generally distributed along clearly defined donkey paths (see Figure 9).

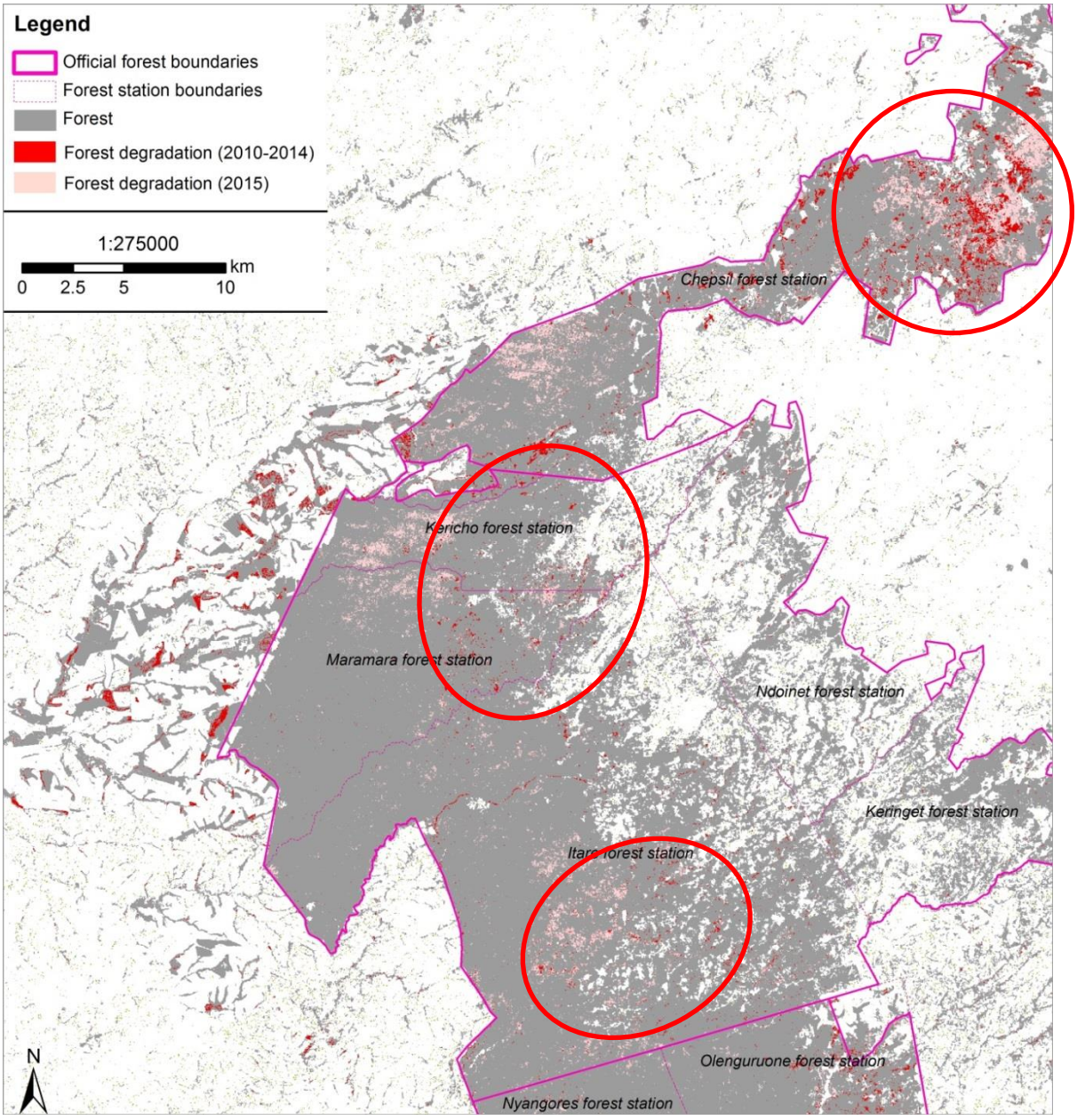

Figure 8: Composite of annual forest degradation maps (2010-2015)

These paths, used to transport charcoal out of the forest, increasingly penetrate the central parts of the south western Mau forest, which becomes a visible trace of forest degradation (see Figure 9 & Figure 10). In general, the study detected most degradation in the western part of the forest. Disturbances in the more eastern bamboo forest parts are less pronounced.

Figure 9: Charcoal kiln used in 2015 and donkey path

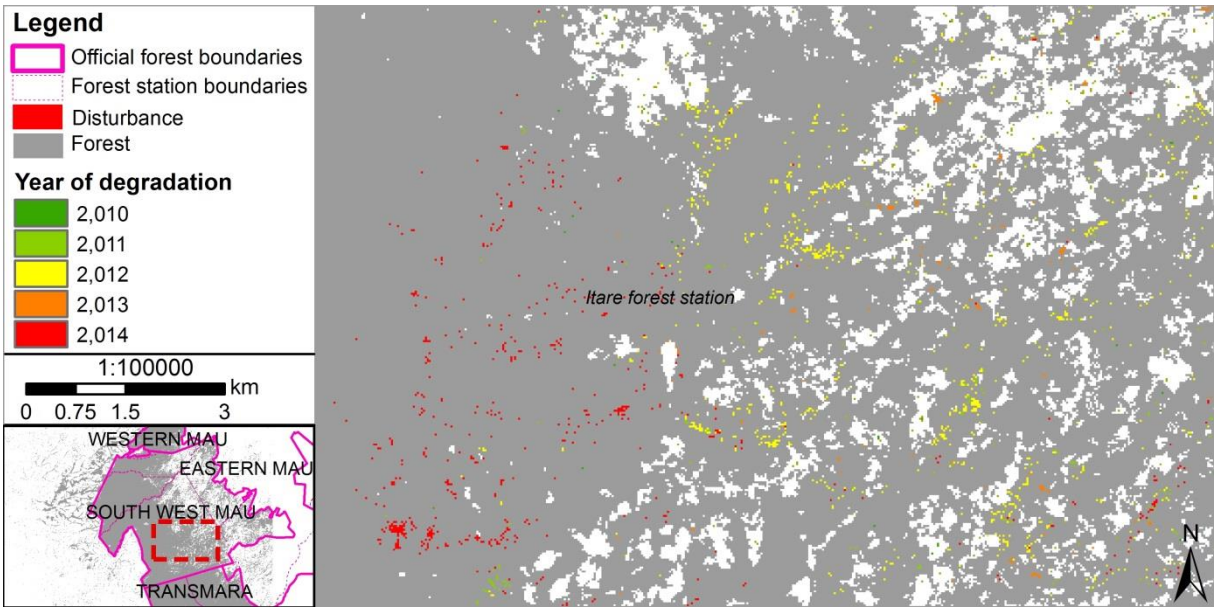

Figure 10: Detailed forest degradation map of central parts of the South Western Mau

4.3 Potential sources of inaccuracies

In comparison to other studies using the NDFI for forest degradation monitoring the method used in this study achieved lower overall accuracies. In Brazil and Indonesia forest degradation has been mapped with an accuracy of around 94 and 95% respectively (Sofan et al. 2016, Souza et al. 2005). These studies used one cloud-free image per year and a simple image differencing algorithm for consecutive time steps. Such an approach, however, is far less promising in the Mau Forest than for tropical rainforests because the Mau Forest is characterized by a mixture of evergreen, semi-deciduous and deciduous trees (Obare and Wangwe 1998). Here cloud-free imagery is only available in the dry season, in which degradation activities are less distinguishable from senescence of the canopy (Miettinen, Stibig and Achard 2014). Especially the leaf-off configuration of some trees, which is absent in tropical rainforests introduces considerable RS signal variation. The combination of high signal variation and very few non-cloudy observations in the rainy season poses an additional challenge to distinguish noise from actual disturbances or seasonal vegetation dynamics. Furthermore, the complex mixture of different forest types (evergreen, semi-deciduous, bamboo) and degradation drivers in the Mau forest may require type-specific configurations of BFAST, which were not implemented in this study. For further accuracy improvement of degradation maps a few more methodological alternatives can be considered:

- investigation and implementation of more sophisticated outlier removal methods
- addition of contextual classification algorithms (CCA) (Souza et al. 2005)
- stratification of BFAST parameters, e.g. based on forest type, topography or distance to settlements

In the framework of this study overall map accuracy was assessed using classes degradation and non-degradation. Generally, the detection of forest degradation worked better for bigger disturbance patches (see Figure 11). Therefore, detection of accuracies could be higher if degradation areas with a size below 0,2 ha are disregarded. In this study no distinction has been made between different drivers of forest degradation. However, it could be observed that logging of single trees (e.g. for honey harvest) is harder to detect than logging at charcoal burning and timber harvesting areas. The latter are characterized by the removal of biomass after disturbance events manifesting as clear drops in the NDFI signature. This drop is much less pronounced when trees remain on the felling location, because less soil is exposed. Potentially the detectability of very low intensity disturbances can be improved with finer resolution RS imagery (Souza Jr, 2013). With 10 m spatial resolution Sentinel 2 imagery is a promising alternative. The satellite additionally outperforms Landsat regarding spectral coverage and temporal resolution. The higher spectral coverage will allow for more accurate modelling of pixel endmember fractions, and therefore result in more accurate NDFI TS. Moreover, the shorter revisit time will provide more dense TS, which has several other advantages:

- better modelling of seasonal signal variations, especially in the rain season
- more accurate outlier detection

- higher detectability of small disturbances followed by understorey regrowth or canopy closure

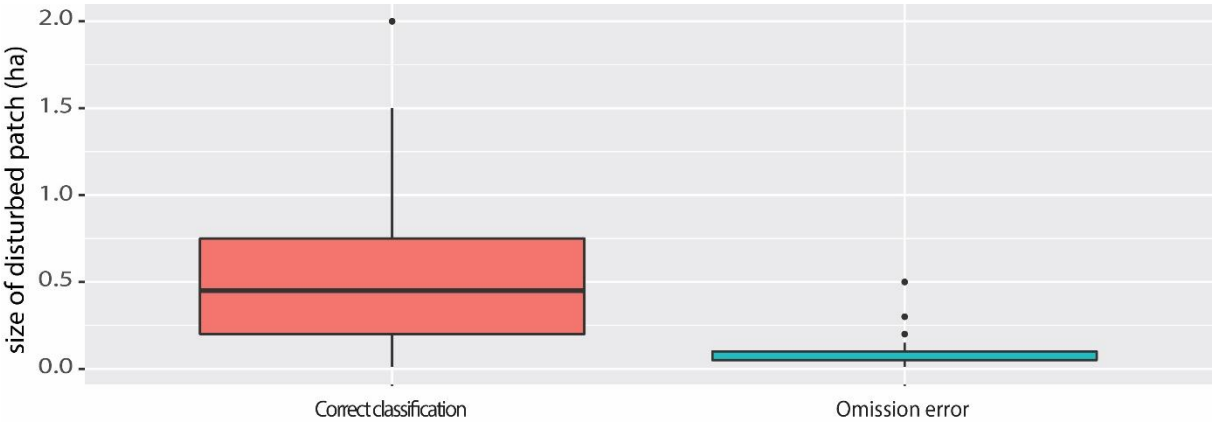

Figure 11: Patch size of detected and undetected degradation areas

Particular difficulties were observed for change detection in 2015. Some mapped degradation patches were unrealistically large in that year, which might explain the large total area of change. Among all monitoring years 2015 demonstrates the lowest precipitation rates for the months between June and September (see Figure 12). Drying out of canopy and understory may have increased the permeability of green vegetation, and the exposure of bare soil and NPV. This causes low NDFI values which potentially were flagged falsely as forest degradation. That becomes apparent through the low producer accuracy of no-degradation pixels, which were thus frequently misinterpreted as disturbed. The implementation of change magnitude and bare soil fraction change thresholds meant to anticipate this issue. Potentially other additional criteria that are more resilient to fluctuations of climate and vegetation phenology could be explored for more reliable breakpoint validation. The exploration of such criteria was not feasible given the time and data availability in this study and remains subject to future research.

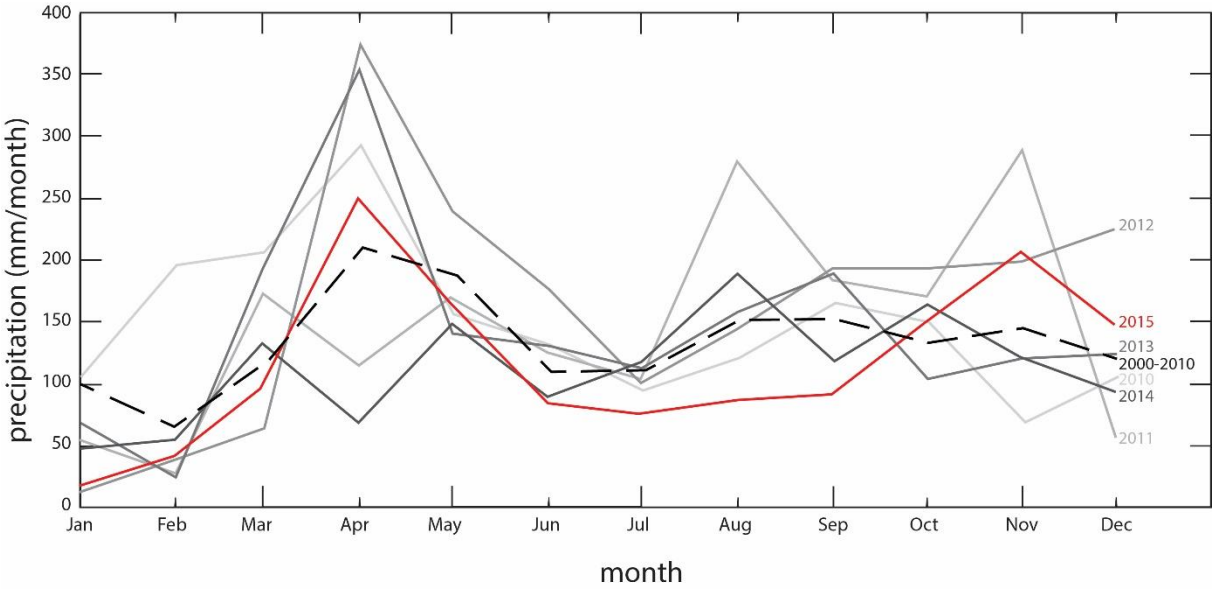

Figure 12: Area-averaged time series of monthly precipitation rate (TRMM data retrieved from Giovanni climate data portal)

4.4 Feasibility for operationalized forest degradation monitoring

The BFAST monitoring algorithm was initially designed for near real-time (NRT) monitoring of deforestation (Verbesselt et al. 2012). Pratihast et al. (2014) developed a BFAST-based framework for continuous deforestation monitoring in the UNESCO Kafa Biosphere Reserve, Ethiopia. Potentially, the method can be also used to operationalize the detection of forest degradation in the Mau Forest. Consistent (free) data acquisition and automated processing procedures pose an effective and cheap way to implement RS-based monitoring systems. To enhance the reliability of such systems ground-based field validation is needed (Li et al. 2013). Field observations may further allow to link locations of forest change to specific dates and drivers of disturbance events. The involvement of local communities and experts is an effective way to establish continuous field data streams, while also addressing REDD+ implementation guidelines. In case of the Mau forest the prospect of paying local community groups and indigenous societies for such services could enhance the surveillance of the forest while at the same time creating a sense of awareness among the local communities.

5 Conclusions

This study is an explorative attempt to apply a BFAST-based algorithm to the challenging task of mapping forest degradation in mixed evergreen and highly seasonal semi-deciduous forests. The use of NDFI provided TS sensitive enough to track most actual forest degradation patches with a size larger than 2 ha. However, the exceptional absence of rainfall in 2015 caused overestimation of degradation in non-disturbed areas. Further research is needed to securely differentiate between phenological anomalies and anthropogenic disturbances.

The research of Schultz (2016) indicates that the combined use of NDFI TS and BFAST is very suitable for the timely detection of deforestation as well. If used in conjunction with deforestation monitoring, this approach could be the base for precise forest monitoring in Kenya. This could enhance the implementation of national MRV systems, and thus may help Kenya to become eligible for the proposed compensation scheme of REDD+.

The findings indicate ongoing disturbances in both at the edge and the interior of the forest, resulting in the continuous fragmentation of the Mau forest. To slow down or reverse this process adequate forest monitoring tools are needed. As human activities progressively shift into the interior of the forest, currently degrading areas cannot be reached within one day. The presented method may support the Kenyan Forest Service and Kenyan Wildlife Service in the planning of patrols, especially when operationalized as an NRT monitoring system. Knowledge on the location and spatial extent of degrading areas may additionally inform policy makers to prioritize main intervention areas.

The advent of the sentinel satellites (S1 and S2) with higher spatial resolution and revisit time marks an interesting opportunity to improve the proposed method. New spectral bands, particularly in the red spectrum, of Sentinel 2 may enhance the distinguishability of tree canopy and understory vegetation. Therefore, the calibration of SMA models may be more

accurate than with Landsat bands, and hence NDFI values more sensitive to small canopy disturbances. For future monitoring it is thus implicit to explore the potential of Sentinel 1 & 2 for forest degradation monitoring.

6 References

Acker, J. G. & G. Leptoukh (2007) Online Analysis Enhances Use of NASA Earth Science Data. Eos, Trans. AGU, Vol. 88, No. 2, 14-17

Adams, J. B., M. O. Smith & A. R. Gillespie (1993) Imaging spectroscopy: Interpretation based on spectral mixture analysis. In Remote geochemical analysis: Elemental and mineralogical composition, eds. V. M. Pieters & P. Englert, 145–166. New York: Cambridge University Press.

Allaway, J. & P. M. J. Cox (1989) Forests and Competing Land Uses in Kenya. Environmental Management, 13, 171-187.

Asner, G. P., M. Keller, R. Pereira & J. C. Zweede (2002) Remote sensing of selective logging in Amazonia - Assessing limitations based on detailed field observations, Landsat ETM+, and textural analysis. Remote Sensing of Environment, 80, 483-496.

Asner, G. P., M. Keller & J. N. M. Silva (2004) Spatial and temporal dynamics of forest canopy gaps following selective logging in the eastern Amazon. Global Change Biology, 10, 765-783.

Broich, M., M. C. Hansen, P. Potapov, B. Adusei, E. Lindquist & S. V. Stehman (2011) Time-series analysis of multi-resolution optical imagery for quantifying forest cover loss in Sumatra and Kalimantan, Indonesia. International Journal of Applied Earth Observation and Geoinformation, 13, 277-291.

Congalton, R. G. (1991) A Review of Assessing the Accuracy of Classifications of Remotely Sensed Data. Remote Sensing of Environment, 37, 35-46.

Coppin, P., I. Jonckheere, K. Nackaerts, B. Muys & E. Lambin (2004) Digital change detection methods in ecosystem monitoring: a review. International Journal of Remote Sensing, 25, 1565-1596.

de Wasseige, C. & P. Defourny (2004) Remote sensing of selective logging impact for tropical forest management. Forest Ecology and Management, 188, 161-173.

DeVries, B., J. Verbesselt, L. Kooistra & M. Herold (2015) Robust monitoring of small-scale forest disturbances in a tropical montane forest using Landsat time series. Remote Sensing of Environment, 161, 107-121.

bfastSpatial: Utilities to monitor for change on satellite image time-series. 0.6.1.

Gaveau, D. L. A., S. Sloan, E. Molidena, H. Yaen, D. Sheil, N. K. Abram, M. Ancrenaz, R. Nasi, M. Quinones, N. Wielaard & E. Meijaard (2014) Four Decades of Forest Persistence, Clearance and Logging on Borneo. Plos One, 9.

GFC. 2010. Getting to the Roots: Underlying Causes of Deforestation and Forest Degradation, and Drivers of Forest Restoration. 42. Asunción, Paraguay: Global Forest Coalition.

Griffiths, P., D. Muller, T. Kuemmerle & P. Hostert (2013) Agricultural land change in the Carpathian ecoregion after the breakdown of socialism and expansion of the European Union. Environmental Research Letters, 8.

Hansen, M. C. & T. R. Loveland (2012) A review of large area monitoring of land cover change using Landsat data. Remote Sensing of Environment, 122, 66-74.

Hirschmugl, M., M. Steinegger, H. Gallaun & M. Schardt (2014) Mapping Forest Degradation due to Selective Logging by Means of Time Series Analysis: Case Studies in Central Africa. Remote Sensing, 6, 756-775.

Huang, C. Q., S. N. Goward, J. G. Masek, F. Gao, E. F. Vermote, N. Thomas, K. Schleeweis, R. E. Kennedy, Z. L. Zhu, J. C. Eidenshink & J. R. G. Townshend (2009) Development of time series stacks of Landsat images for reconstructing forest disturbance history. International Journal of Digital Earth, 2, 195-218.

Imo, M. 2012. Forest Degradation in Kenya: Impacts of Social, Economic and Political Transitions. In Kenya: political, social and environmental issues, eds. J. W. Adoyo & C. I. Wangai, 1-38. New York: Nova Science Publishers.

Leisch, F., Hornik, K., & Kuan, C. (2000). Monitoring structural changes with the generalized fluctuation test. Econometric Theory, 16, 835–854.

Li, X., S. Wang, Y. Ge, R. Jin, S. Liu, M. Ma, W. Shi, R. Li & Q. Liu. (2013). Development and experimental verification of key techniques to validate remote sensing products. In International Archives of the Photogrammetry, Remote Sensing and Spatial Information Sciences, 25-30. Hong Kong: Remote Sensing Spatial Information Science.

Margono, B. A., S. Turubanova, I. Zhuravleva, P. Potapov, A. Tyukavina, A. Baccini, S. Goetz & M. C. Hansen (2012) Mapping and monitoring deforestation and forest degradation in Sumatra (Indonesia) using Landsat time series data sets from 1990 to 2010. Environmental Research Letters, 7.

Miettinen, J., H.-J. Stibig & F. Achard (2014) Remote sensing of forest degradation in Southeast Asia—Aiming for a regional view through 5–30 m satellite data. Global Ecology and Conservation, 2, 24-36.

Mogaka, H., S. Gichere, R. Davis & R. Hirji. 2006. Climate Variability and Water Resources Degradation in Kenya: Improving Water Resources Development and Management. In World Bank Working Paper Washington, D.C.: The International Bank for Reconstruction and Development/The World Bank.

Obare, L. & J. B. Wangwe. 1998. Underlying Causes of Deforestation and Forest Degradation in Kenya. ed. W. R. Movement.

Olang, L. U. & P. M. Kundu. 2011. Land Degradation of the Mau Forest Complex in Eastern Africa: A Review for Management and Restoration Planning, . In Environmental Monitoring, ed. E. Ekundayo. InTech.

Pfaff, A. S. P. (1999) What drives deforestation in the Brazilian Amazon? Evidence from satellite and socioeconomic data. Journal of Environmental Economics and Management, 37, 26-43.

Pratihast, A. K., B. DeVries, V. Avitabile, S. de Bruin, L. Kooistra, M. Tekle & M. Herold (2014) Combining Satellite Data and Community-Based Observations for Forest Monitoring. Forests, 5, 2464-2489.

Pratihast, A. K., M. Herold, V. Avitabile, S. de Bruin, H. Bartholomeus, C. M. Souza & L. Ribbe (2013) Mobile Devices for Community-Based REDD+ Monitoring: A Case Study for Central Vietnam. Sensors, 13, 21-38.

R: A language and environment for statistical computing. R Foundation for Statistical Computing. 3.0.2, Vienna, Austria.

Schultz, M., Clevers, J. G.P.W., Carter, S., Verbesselt, J., Avitabile, V., Quang, H.V. & Herold, M. (2016). International Journal of Applied Earth Observation and Geoinformation. In review

Sharife, K. 2010. REDD: Seeing the Forest for the Trees. In Huff Post Green. Huff Post.

Sofan, P., Y. Vetrita, F. Yulianto & M. R. Khomarudin (2016) Multi-temporal remote sensing data and spectral indices analysis for detection tropical rainforest degradation: case study in Kapuas Hulu and Sintang districts, West Kalimantan, Indonesia. Natural Hazards, 80, 1279-1301.

Souza, C. M. & D. Roberts (2005) Mapping forest degradation in the Amazon region with Ikonos images. International Journal of Remote Sensing, 26, 425-429.

Souza, C. M., D. A. Roberts & M. A. Cochrane (2005) Combining spectral and spatial information to map canopy damage from selective logging and forest fires. Remote Sensing of Environment, 98, 329-343.

Souza Jr, C. M., J. V. Siqueira, M. H. Sales, A. V. Fonseca, J. G. Ribeiro, I. Numata, M. A. Cochrane, C. P. Barber, D. A. Roberts & J. Barlow (2013) Ten-year landsat classification of deforestation and forest degradation in the brazilian amazon. Remote Sensing, 5, 5493-5513.

Stueve, K. M., I. W. Housman, P. L. Zimmerman, M. D. Nelson, J. B. Webb, C. H. Perry, R. A. Chastain, D. D. Gormanson, C. Huang, S. P. Healey & W. B. Cohen (2011) Snow-covered Landsat time series stacks improve automated disturbance mapping accuracy in forested landscapes. Remote Sensing of Environment, 115, 3203-3219.

Unknown (2002) Forests excision could turn Kenya into desert. In ogiek.org.

Verbesselt, J., R. Hyndman, G. Newnham & D. Culvenor (2010a) Detecting Trend and Seasonal Changes in Satellite Image Time Series. Remote Sensing of Environment, 114, 106-115.

Verbesselt, J., R. Hyndman, A. Zeileis & D. Culvenor (2010b) Phenological change detection while accounting for abrupt and gradual trends in satellite image time series. Remote Sensing of Environment, 114, 2970-2980.

Verbesselt, J., A. Zeileis & M. Herold (2012) Near real-time disturbance detection using satellite image time series. Remote Sensing of Environment, 123, 98-108.

Author. 2009. Redd in Africa: How we can earn money from air by harvesting carbon. The Guardian October 5.

Were, K. O., O. B. Dick & B. R. Singh (2013) Remotely sensing the spatial and temporal land cover changes in Eastern Mau forest reserve and Lake Nakuru drainage basin, Kenya. Applied Geography, 41, 75-86.

WildlifeDirect. 2010. How sugarcane might save the Mau Forest. In Mau Mandala.

Wulder, M. A., J. G. Masek, W. B. Cohen, T. R. Loveland & C. E. Woodcock (2012) Opening the archive: How free data has enabled the science and monitoring promise of Landsat. Remote Sensing of Environment, 122, 2-10.

Zhu, Z. & C. E. Woodcock (2012) Object-based cloud and cloud shadow detection in Landsat imagery. Remote Sensing of Environment, 118, 83-94.

7 Appendix

Annex 1: Processing chain

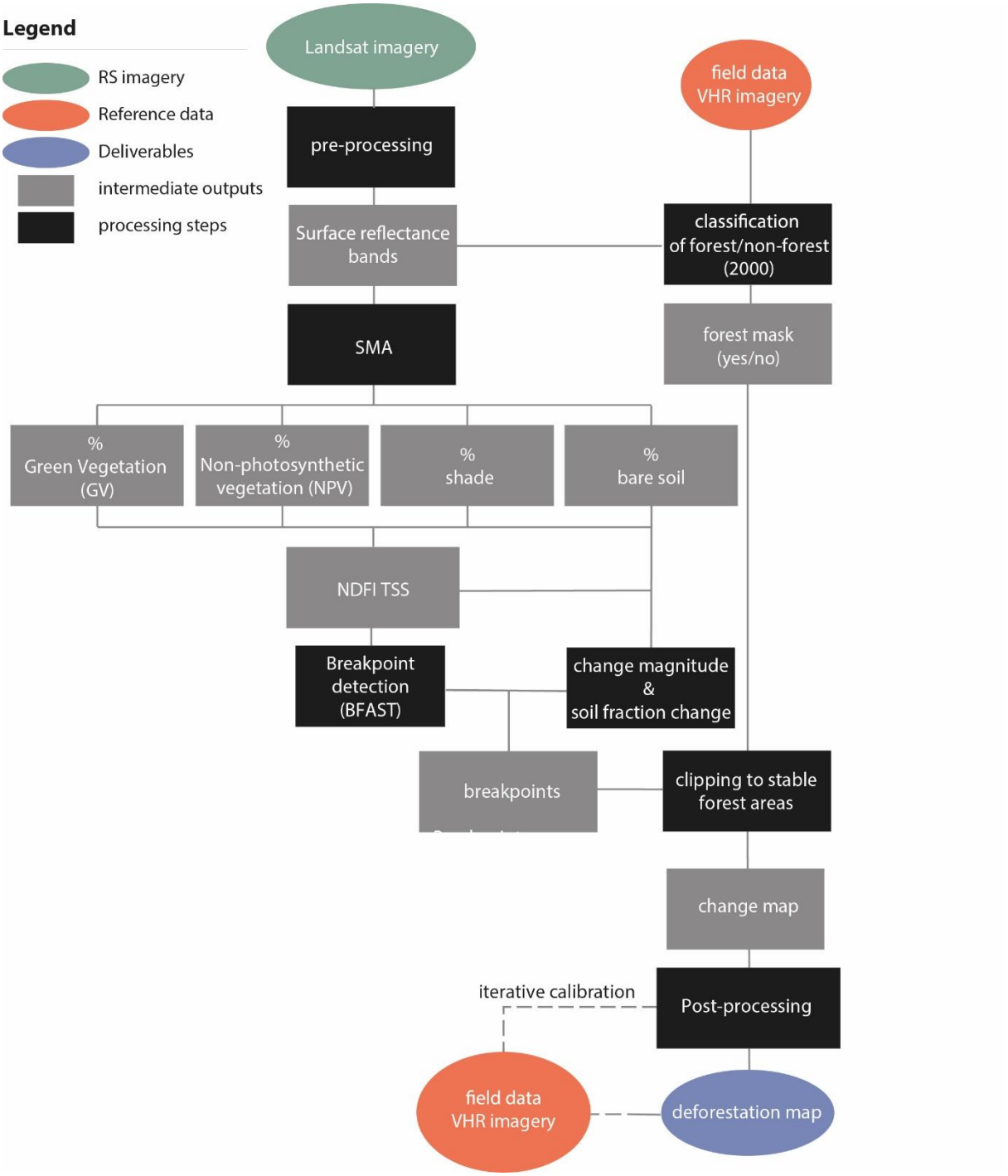

Annex 2: Geographic extent of overlap zones

Zone	Xmin	Xmax	Ymin	ymax	Overlapping tiles
NW	Xmin (170-60)	Xmax (170-60)	Ymax (169_61)	Ymax (169-60)	170-60, 169-60
NE	Xmax (170-60)	Xmax (169-60)	Ymax (169_61)	Ymax (169-60)	169-60
SW	Xmin (170-60)	Xmax (170-60)	Ymin (169_61)	Ymax (169_61)	170-60, 169-60, 169-61
SE	Xmax (170-60)	Xmax (169-60)	Ymin (169_61)	Ymax (169_61)	169-60, 169-61

Annex 3: Sampling and accuracy assessment procedures

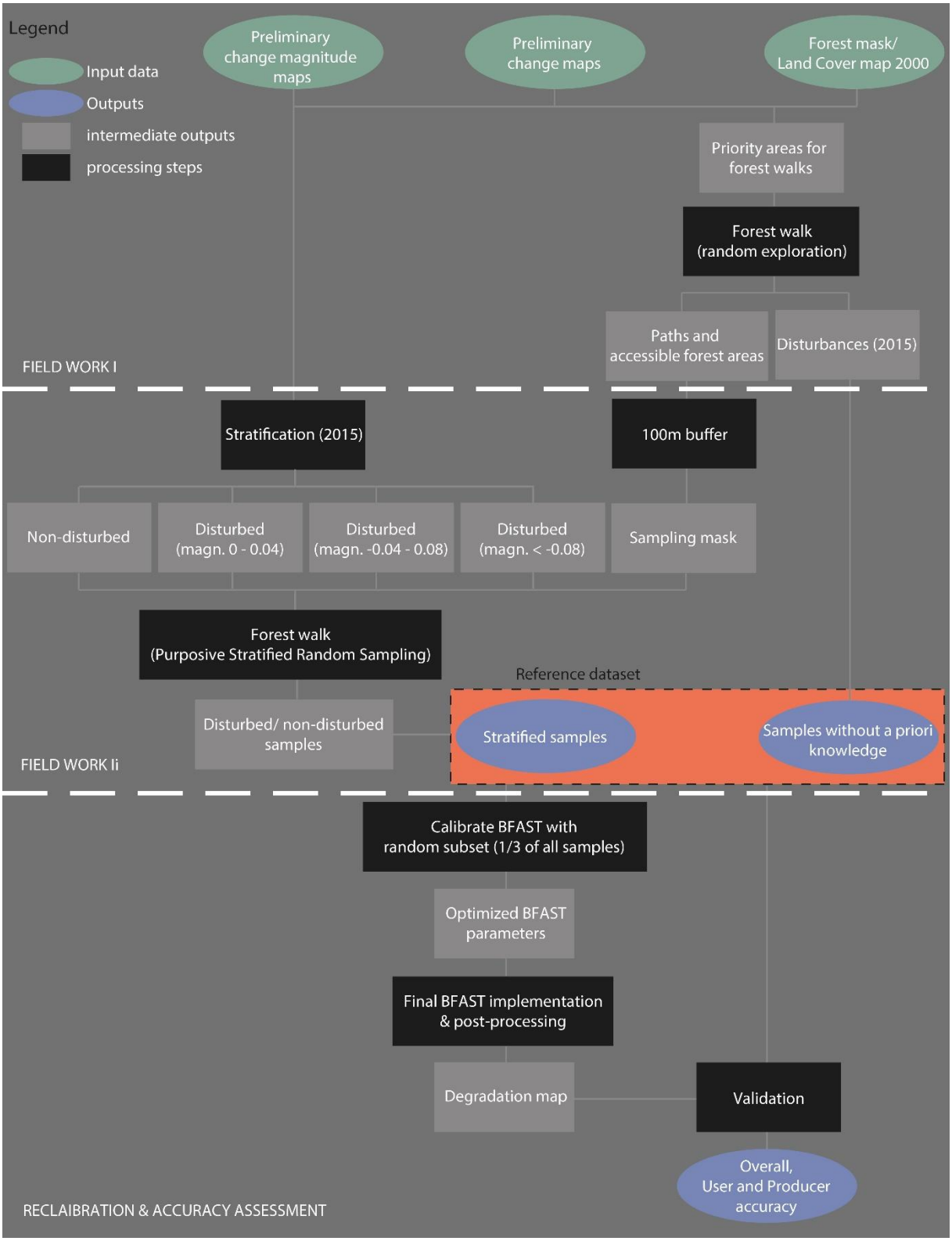

Annex 4: Stable forest mask

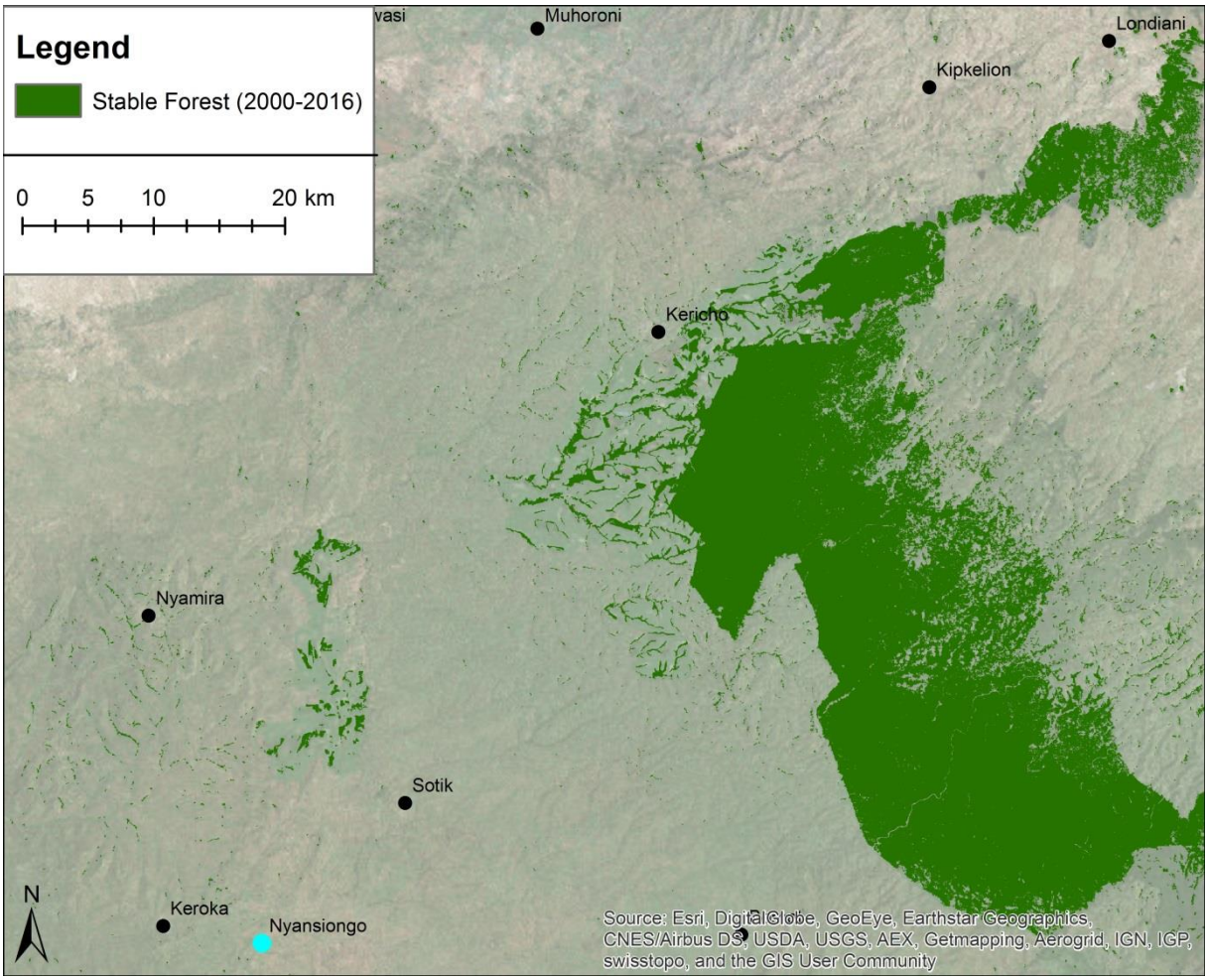

Annex 5: Annual forest degradation maps for the years 2010-2015

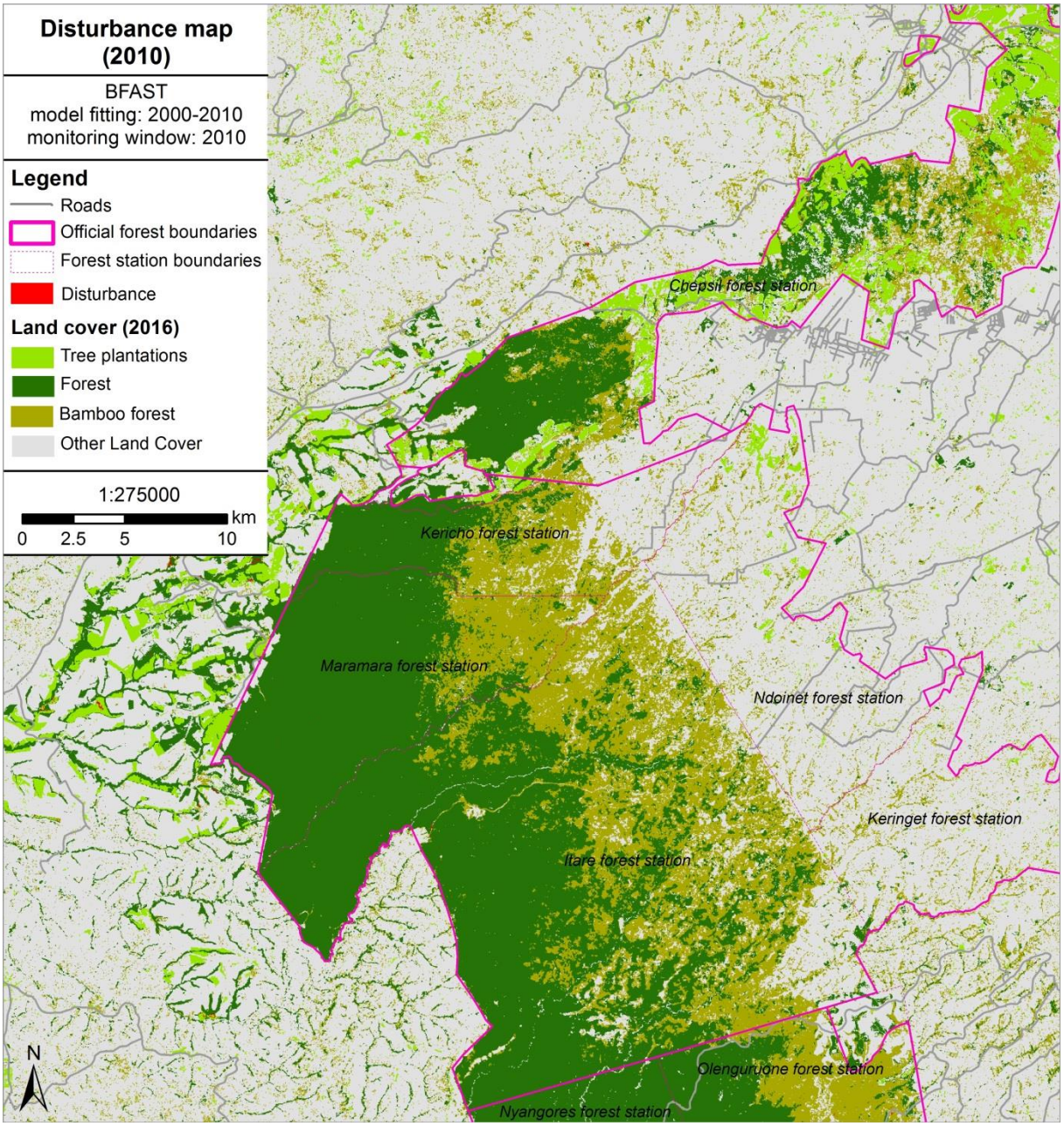

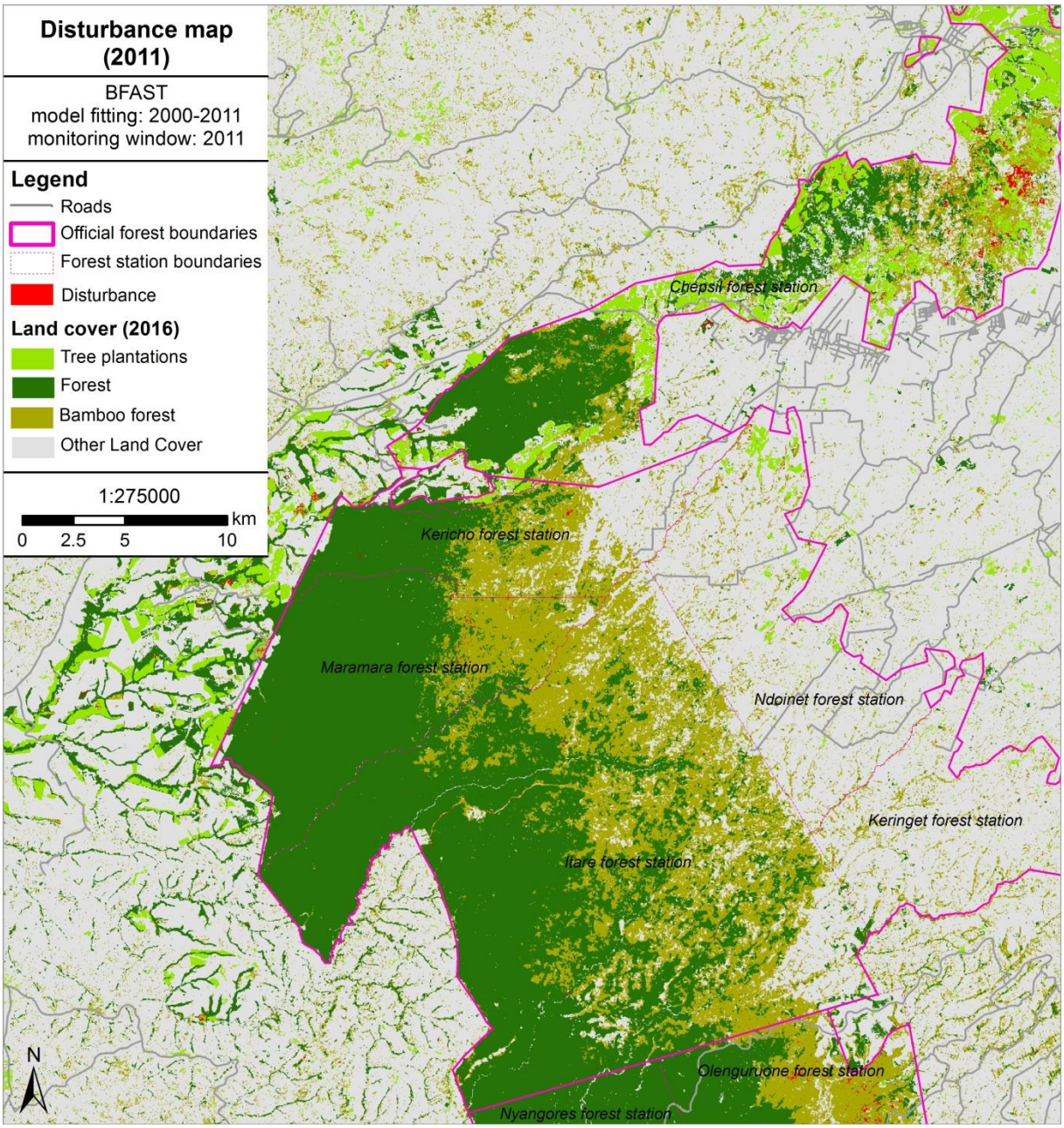
Disturbance map (2011)
BFAST
model fitting: 2000-2011
monitoring window: 2011
Legend
Roads
Official forest boundaries
Forest station boundaries
Disturbance
Land cover (2016)
Tree plantations
Forest
Bamboo forest
Other Land Cover
1:275000
0 2.5 5 10 km
N
Chepsir forest station
Kericho forest station
Maramara forest station
Ndoinet forest station
Keringet forest station
Itare forest station
Olenguruone forest station
Nyangores forest station

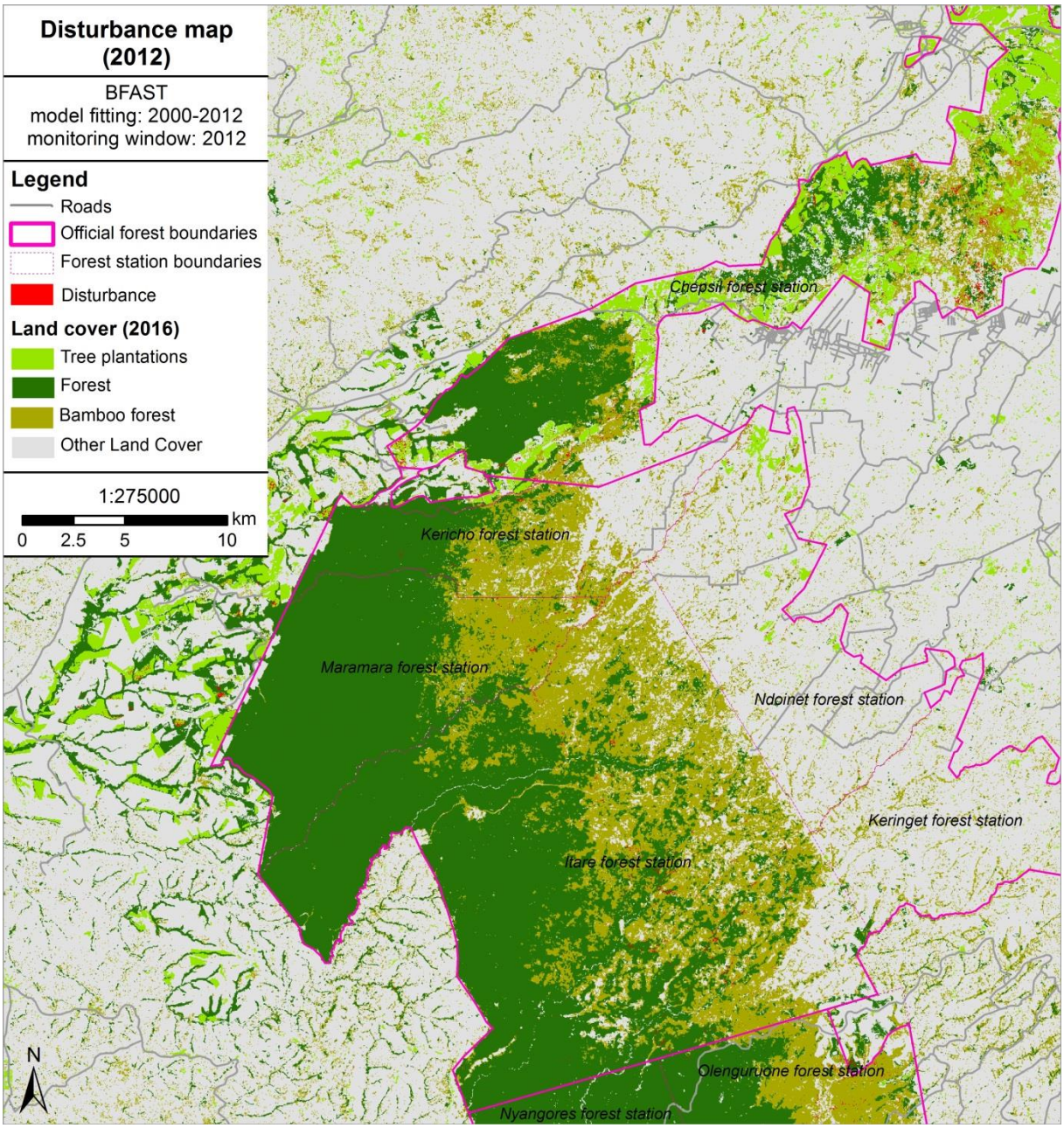
Disturbance map (2012)
BFAST
model fitting: 2000-2012
monitoring window: 2012
Legend
Roads
Official forest boundaries
Forest station boundaries
Disturbance
Land cover (2016)
Tree plantations
Forest
Bamboo forest
Other Land Cover
1:275000
0 2.5 5 10 km
N
Chepsir forest station
Kericho forest station
Maramara forest station
Ndoinet forest station
Keringet forest station
Itare forest station
Olenguruone forest station
Nyangores forest station

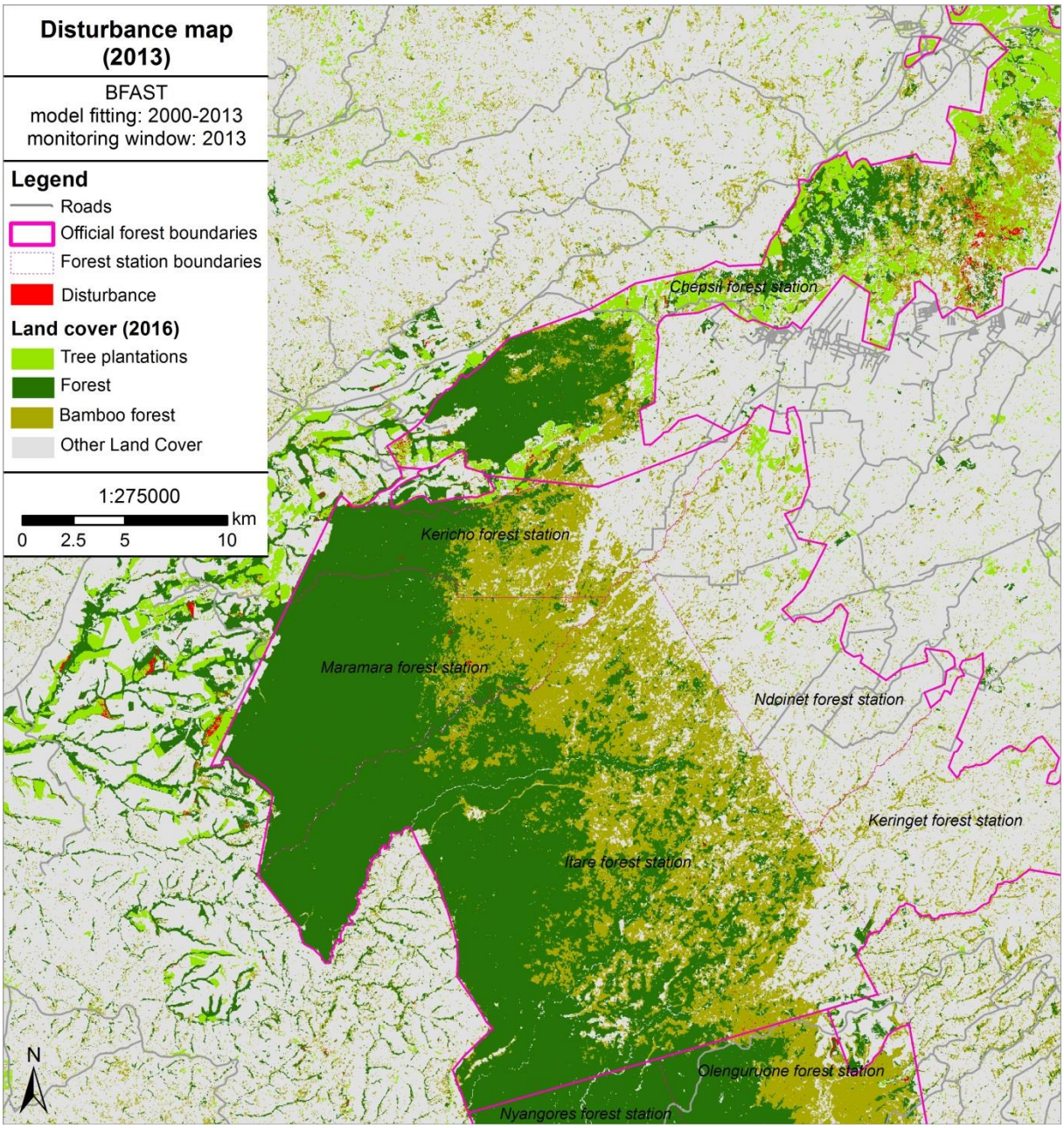
Disturbance map (2013)
BFAST
model fitting: 2000-2013
monitoring window: 2013
Legend
Roads
Official forest boundaries
Forest station boundaries
Disturbance
Land cover (2016)
Tree plantations
Forest
Bamboo forest
Other Land Cover
1:275000
0 2.5 5 10 km
N
Chepsir forest station
Kericho forest station
Maramara forest station
Ndoinet forest station
Keringet forest station
Itare forest station
Olenguruone forest station
Nyangores forest station

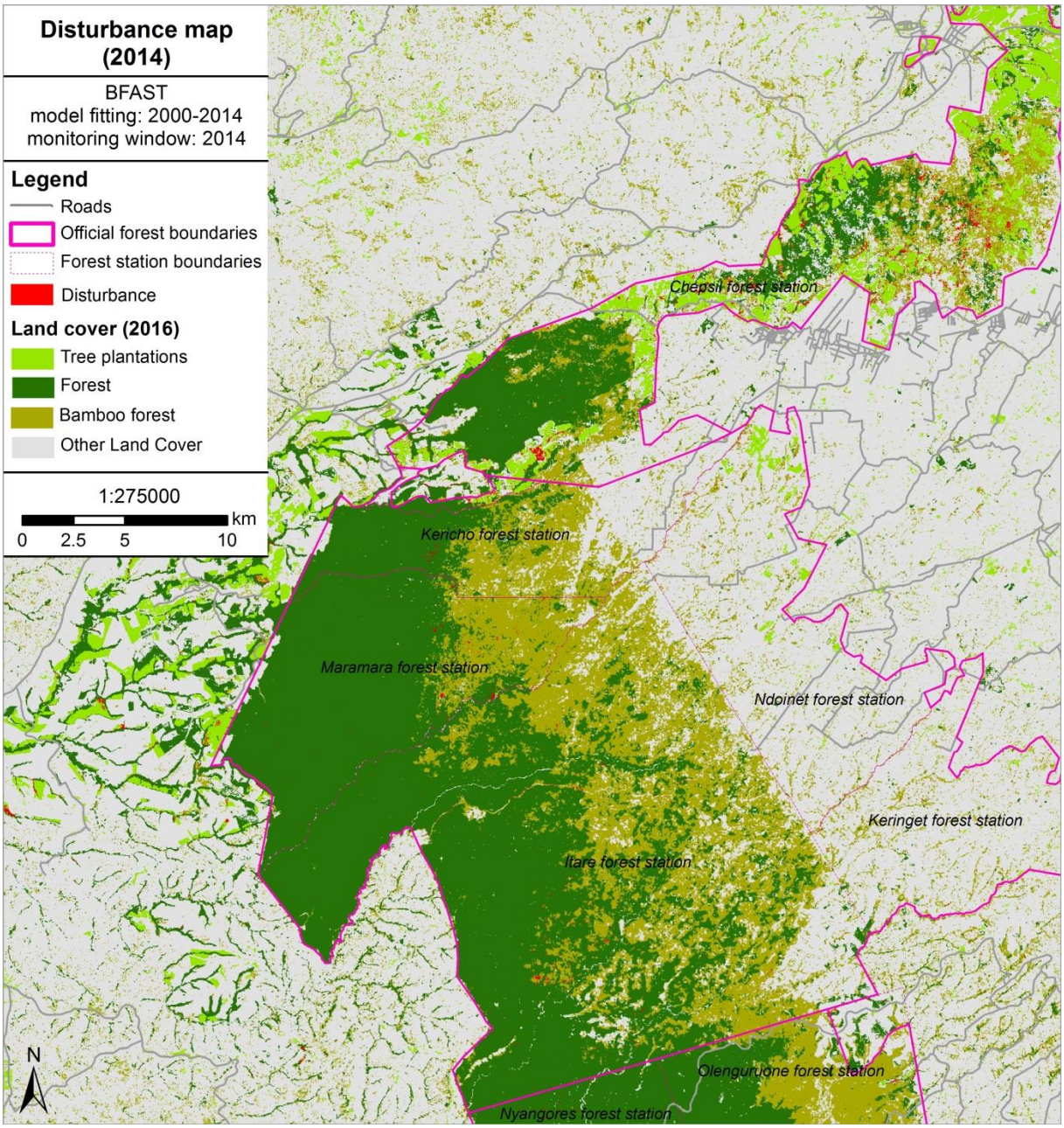
Disturbance map (2014)
BFAST
model fitting: 2000-2014
monitoring window: 2014
Legend
Roads
Official forest boundaries
Forest station boundaries
Disturbance
Land cover (2016)
Tree plantations
Forest
Bamboo forest
Other Land Cover
1:275000
0 2.5 5 10 km
N
Chepsir forest station
Kericho forest station
Maramara forest station
Ndoinet forest station
Keringet forest station
Itare forest station
Olenguruone forest station
Nyangores forest station

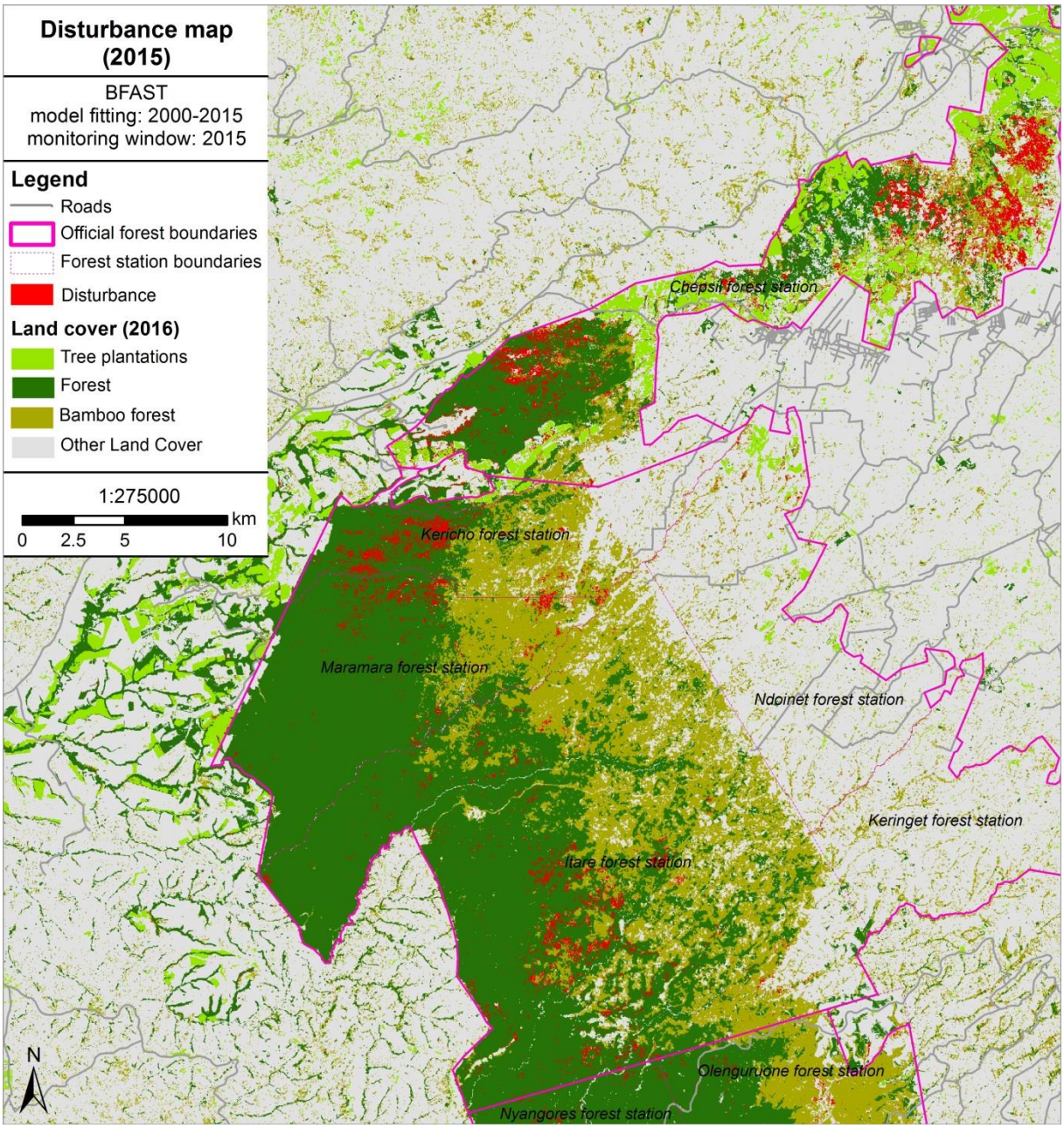
Disturbance map (2015)
BFAST
model fitting: 2000-2015
monitoring window: 2015
Legend
Roads
Official forest boundaries
Forest station boundaries
Disturbance
Land cover (2016)
Tree plantations
Forest
Bamboo forest
Other Land Cover
1:275000
0 2.5 5 10 km
N
Chepsir forest station
Kericho forest station
Maramara forest station
Ndoinet forest station
Keringet forest station
Itare forest station
Olenguruone forest station
Nyangores forest station